CHAPTER 3: CHARACTERIZATION OF THE SFBR EARTHQUAKE SOURCES

Introduction

This chapter summarizes the geologic data for the characterized sources of SFBR: the San Gregorio, San Andreas, Hayward-Rodgers Creek, Calaveras, Greenville, Concord-Green Valley faults and the Mt. Diablo thrust (**Figure 3.1**). These data, to be used as input in the Calculation Sequence of the following chapter, include:

1) Fault Segmentation. The 18 fault segments defined in this study are the basic building blocks of the SFBR earthquake model. Segments and the uncertainty in segment end points are shown in **Figure 3.1**. Segment names and their acronyms are listed in **Table 3.1**.

2) Geologic Slip Rates. These determine the average rates of earthquakes as given by the SFBR earthquake model. Geologic slip rates are typically averaged over time periods of hundreds to several tens of thousands of years.

3) Previous Earthquakes: Recurrence and Slip per Event. Recurrence interval data obtained from the paleoseismic record provide important checks on recurrence intervals resulting from the SFBR earthquake model, but such data are sparse for SFBR faults. Timing of the most recent event (MRE) is essential for all of the time-dependent probability models; the MRE displacements are needed in addition for the time-predictable model.

4) Rupture Sources, Rupture Scenarios, and Fault-Rupture Models. These are new concepts developed for this analysis to allow for all possible combinations of earthquake rupture along faults comprised of two or more segments.

5) Data for Determining Fault Area (A). Estimates are summarized for segment or fault width (W), the length of the down-dip extent of the fault from the surface to the base of the seismogenic crust (Appendix A), and the seismogenic slip factor R for each segment (Appendices B and C). Together with segment lengths (L), these quantities determine segment areas A.

Much of these data can be assembled from the available literature, but the fault segmentation and fault-rupture models presented here are the products of three source-characterization groups (SCG) convened for this purpose. The first of these groups (San Andreas SCG) dealt with the San Andreas and San Gregorio faults, the second (East Bay SCG) with the four East Bay strike-slip faults, and the third (Thrust and Reverse SCG) with regional thrust and reverse faults. These groups were also charged with evaluating newly available data in the context of the existing literature. Each group was composed of geologists, geodecists, seismologists, and geophysicists with expert knowledge of the specific faults and/or the general earthquakesprocess. Each group met in a series of workshops, which led to development of the source characterization inputs presented here. Participants in these groups are listed in Appendix A

Table 3.1 SFBR segments names and acronyms.

Fault	Seg.	Segment Name
San Andreas	SA0	Offshore
	SAN	North Coast
	SAP	Peninsula
	SAS	Santa Cruz Mountains
Hayward/Rodgers Creek	RC	Rodgers Creek
	HN	Northern Hayward
	HS	Southern Hayward
Calaveras	CN	Northern Calaveras
	CC	Central Calaveras
	CS	Southern Calaveras
Concord/Green Valley	GVN	Northern Green Valley
	GVS	Southern Green Valley
	CON	Concord
San Gregorio	SGN	Northern San Gregorio
	SGS	Southern San Gregorio
Greenville	GN	Northern Greenville
	GS	Southern Greenville
Mount Diablo Thrust	MTD	No segments

FAULT SEGMENTATION

Fault Segments, Rupture Sources, Rupture Scenarios, and Rupture Models

A *fault segment* is the basic building block for each fault, the shortest section considered capable of repeatedly rupturing to produce the large earthquakes of interest here. Fault segments are identified according to two criteria: kinematic considerations, such as geometry and structure, and dynamic considerations, such as timing, rupture length, and displacements of previous earthquakes Kinematic considerations include changes in strike, the occurrence of restraining bends or extensional steps, branching or intersection points, changes in fault complexity, and major changes in lithology along the fault. Because earthquakes may respect none of these features, kinematic segmentation alone can be uncertain. Most important of the dynamic considerations are differences in timing of events on adjacent parts of a fault based on paleoseismic dates and/or historical ruptures. Changes in fault slip rate, the distribution and nature of microearthquake activity, and the transition to or changes in the rate of creep along a fault are also indicators of potential segmentation points. Within the limits of the available data all of these indicators were utilized to identify the fault segments presented here. The *floating earthquake* is also introduced as part of the fault characterization. This is an earthquake, with magnitude and length fixed by the historical record, that can occur on a fault at locations other than the segments defined in the current characterization.

If SFBR earthquakes arose only from single-segment ruptures, making and counting earthquakes in the slip-rate balanced format of the SFBR earthquake model would be a straightforward calculation. Indeed, this was the basis for the WG90 report, calculating single-segment rupture

rates and probabilities for the three segments of the Hayward-Rodgers Creek fault and three segments of the San Andreas fault. The geologic evidence is clear, however, that multiple-segment ruptures can and do occur in the SFBR, most recently during the 1906 earthquake in which all three of the WG90 segments, and all four of the segments that comprise the San Andreas fault in this study, ruptured.

WG02 differs from WG 90 not only in the definition and characterization of the fault segments, but in allowing multiple segment ruptures. To accommodate multiple segment ruptures WG 99 introduced the concepts of *rupture source*, *rupture scenario*, and *rupture model.* The Hayward-Rodgers Creek fault serves as an example for these **(Figure 3.2)**. A *rupture source* is a single fault segment, or a combination of two or more adjacent segments, that produces an earthquake. For the Hayward- Rodgers Creek fault there are three rupture segments: southern Hayward (HS), northern Hayward (HN), and Rodgers-Creek (RC) **(Figure 3.2a).** The Hayward-Rodgers Creek fault, then, has six possible, *rupture sources:* three single-segment rupture sources (HS, HN, and RC), two two-segment rupture sources (HS+HN and HN+RC) and one three-segment rupture source (HS+HN+RC) **(Figure 3.2b).** Slip in multiple segment ruptures is larger than in the corresponding set of single-segment ruptures. An important consequence of allowing for multiple-segment ruptures, then, is that larger their larger slip reduces the rates of single-segment ruptures. In addition to these characterized rupture sources, floating earthquakes of **M** = 6.9 can occur anywhere along the Hayward-Rodgers Creek fault.

A *rupture scenario* is a combination of *rupture sources* that describes a possible mode of failure of the entire fault during one earthquake cycle. For the Hayward-Rodgers fault, there are four characterized fault-rupture scenarios: 1) HS, HN, and RC as single-segment ruptures; 2) SH as a single-segment rupture and HN+RC as a two-segment rupture; 3) RC as a single-segment rupture and SH+HN as a two-segment rupture; and 4) HS+HN+RC as a three-segment rupture **(Figure 3.2c)**. A fifth fault-rupture scenario is the entire Hayward-Rodgers Creek fault failing only as a result of the floating earthquakes.

Fault-rupture models are weighted combinations, expressing the expert opinion of the appropriate source-characterization group, of the fault-rupture scenarios. Each rupture model is a proposed representation of the long-term behavior of the fault. Specifically, group members were asked the following question: If the entire length of a fault failed completely 100 times, what would be the frequency (percentage) of each rupture scenario? Fault rupture models for the Hayward-Rodgers Creek fault, with weights assigned to each scenario and to each model, are illustrated in **Figure 3.2d**. These models reflect the considered opinion of the source characterization groups about the strength and persistence of segmentation points. For example, if dates of historical and paleoearthquakes indicated that different parts of the fault had ruptured at distinctly different times, and if there were geometric changes associated with these locations, then a rupture model would likely contain a higher percentage of rupture scenarios with individual segments. If dates of paleoearthquakes along the fault overlapped, or if geometric changes were minor, this would be reflected by a rupture model that allowed for a larger percentage of multi-segment ruptures.

The product of rupture scenario and model weights provides a general estimate of the mean rate of occurrence of each rupture source (different size earthquakes) for each of the characterized

SFBR faults. However, both earthquake size and fault slip rate affect the straightforward calculation of recurrence in this way. For example, Hayward-Rodgers Creek rupture scenario 3 contains two ruptures sources--a single segment source (RC) and a multi-segment source (HN+HS) **(Figure 3.2b)**. Because the HN+HS source is longer it produces a larger earthquake with more slip, and the RC segment must fail more frequently given that the slip rate is constant along the fault length. To account for this, slip rates must be applied to the rupture scenarios for the purpose of recalculating frequency of rupture, a process referred to as moment balancing (**Chapter 4**). Complexity is added for faults that have variable slip rates along their length such as the San Andreas and the Calaveras, and by including a floating earthquake.

The moment balancing used in the rupture frequency calculations was developed and applied after the source characterization groups had completed their efforts. Because of this, the SCG's did not have the opportunity to review and compare the moment-balanced results. Rather than reconstitute the SCG's for this purpose, a subset of the Overview Group compared the rupture frequencies from the weighted source characterization models to those calculated after the moment-balancing step (**Appendix G**). While there are small differences, the overall intent of the characterization groups with regard to the behavior of each fault has been maintained through this process.

SOURCE CHARACTERIZATION OF THE SFBR FAULTS

San Andreas Fault

The San Andreas fault alone accounts for more than half of the geologic slip rate across SFBR and more than 90% of the SFBR seismic moment sum in the historical record. Three of the four historical SFBR $M \geq 6.7$ earthquakes (1838, 1906, and 1989) have occurred on or near the San Andreas fault. The 470-km rupture length of the 1906 earthquake is, by far, the longest known surface rupture for strike-slip earthquakes in continental crust.

Segmentation

WG 90 divided the San Andreas fault into three segments: the North Coast, Peninsula, and southern Santa Cruz Mountains segments. The basis for this was a combination of data from the 1838, 1906, and1989 earthquakes, variability in the distribution of geodetically determined slip in the 1906 earthquake (Thatcher and Lisowski, 1987), and changes in the strike of the fault. The North Coast segment was considered to fail only in 1906-type ruptures. The likely occurrence of the 1838 earthquake along the fault on the San Francisco peninsula suggested the existence of the Peninsula segment, with a southern boundary at the north end of the Loma Prieta aftershock zone and a northern boundary at Lower Crystal Springs Reservoir. The latter location is the site of a 5° releasing bend and is also where slip in 1906 was geodetically inferred to decrease from 4 m to 2.5 m. WGNCEP 96 and Petersen and others (1996) concluded that the north end of the Peninsula segment should be near the Golden Gate to reflect the revised 1906 geodetic slip distribution (Thatcher *and others*, 1997) which moved the major decrease in displacement from Lower Crystal Springs Reservoir to a point offshore of the Golden Gate.

Consistent with WGNCEP 96 segmentation, the San Andreas SCG divided the San Andreas fault into four major segments: Offshore (SAO), North Coast (SAN), Peninsula (SAP), and Santa Cruz Mountains (SAS). The segments and their boundaries are shown in **Figure 3.1** and **Figure 3.3.**

SAO. The 135-km long SAO segment subdivides the 1906 rupture north of the Golden Gate. Little is known about this part of the fault because it is largely offshore. The northern boundary is at the geodetically-determined end of the 1906 rupture (Thatcher and others,1997), and the southern boundary is placed in a ± 5 km long zone offshore of Pt. Arena, where a 10-15° change in the strike of the fault occurs. The 1898 earthquake (**M** = 6.8) produced extensive damage along the Mendocino County coast and may have occurred on the southern part of SAO (Bakun, 2000). Thatcher and others (1997) inferred a step in 1906 displacements near Pt. Arena and increasing fault slip to the northwest.

SAN. The SAN segment extends 191 km from Pt. Arena to offshore of the Golden Gate, where a structurally complex intersection between the San Andreas and San Gregorio faults is located. Here, a 3-km right-releasing step along the San Andreas fault is inferred from aeromagnetic, seismic-reflection, and seismicity data (Jachens and Zoback, 1999; Zoback *et.al*., 1999). Slip in the 1906 earthquake decreases from an average of 5.3 ± 0.3m north of the Golden Gate to 3.3 ± 0.3 m on the Peninsula (Thatcher, 1999) (**Figure 3.4).** There is also a change in the geologic slip rate, with the late-Holocene rate decreasing southward across the Golden Gate from 24 mm/yr to 17 mm/yr (Schwartz *and others*, 1998; Hall and others, 1999). The 1906 event is thought to have nucleated in this area. An uncertainty of ±15 km is assigned to the south end of this segment (**Figure 3.1**).

SAP. The Peninsula segment extends 85 km from the Golden Gate southeast to Los Gatos. The southern end lies in a broad zone (±10 km) coincident with a restraining bend in the fault, the north end of the Loma Prieta aftershock zone, and a major lithologic change defined by the north end of the Logan Gabbro. The 1838 earthquake has been located on this part of the San Andreas fault (Louderback, 1947; WG 88, WG 90). Toppozada and Borchardt (1998) concluded that the 1838 event occurred on the Peninsula and Santa Cruz Mountains segments with a magnitude of 7.5. They based this on intensity data at Monterey (MMI VI) only and interpreted this intensity as requiring a rupture form Golden Gate to San Jaun Bautista. Using the same intensity reports, Bakun (1999) interpreted the Peninsula segment as a high probability location, but estimated the M to be 6.8. Paleoseismic studies at the Filoli site allow the possibility that 1.6 m of offset occurred during an earthquake that post-dates 1650, which could be 1838 slip (Hall and others, 1999). While it seems reasonable that the 1838 earthquake occurred on the Peninsula segment, there are no unequivocal observations placing the 1838 event on the San Andreas fault.

SAS. This 62 km-long segment extends from Los Gatos to San Juan Bautista, where the transition to aseismic slip occurs. SAN is similar in length to that delineated by WG90, WGNCEP96, and Petersen *and others* (1996). Independent behavior of this segment is indicated by the timing of past events, evidently different from the Peninsula segment to the north. Evidence from Grizzly Flat (Schwartz and others,1998) and Arano Flat (Heingartner and Schwartz,1996; Fumal, and others,1999) indicates that rupture of the 1838 earthquake did not extend into the Santa Cruz Mountains as suggested by Toppozada and Borchardt (1998).

Schwartz and others (1998) concluded that only one surface rupture, that in 1906, has broken this segment of the fault since AD 1640-1659. WG02 considers this section of the San Andreas fault to be distinct from the reverse-oblique source of the 1989 Loma Prieta earthquake.

Other potential segments. The San Andreas SCG also discussed other possible San Andreas segments, most notably one between Pt. Arena and Ft. Ross. Here, a ~50-km-long low in1906 slip has been determined from geodetic data (Thatcher et al, 1997), which is coincident with a similar low in the 1906 surface offsets (Lawson, 1908). Noller and Lightfoot (1997) obtained a minimum late-Holocene slip rate of 16-18 mm/yr based on the displacement of an archaeological site at Fort Ross. Just to the south of Fort Ross, Prentice and others (2001) suggest a preliminary slip of 18 ± 3 mm/yr for the past ~5000 years. If the 24 mm/yr slip rate assigned to the North Coast is uniform across this reach of the fault, the slip low could fill in with an earthquake of about M 7, a magnitude consistent with this length of fault. Having no information on slip in the pre-1906 earthquake and given the slip rate uncertainties, a distinct Ft. Ross segment is not presently defined. The potential for this type of rupture is treated with the use of a floating M 6.9 earthquake.

Slip Rate

WG 90 used a uniform slip rate of 19 ± 4 mm/yr along the length of the 1906 rupture, which was based on geologic rates, geodetic rates, and estimates of slip from the 1906, and1989 earthquakes. Paleoseismic data developed since1990, however, indicate the San Andreas slip rate decreases south of the Golden Gate (WGNCEP, 1996; Schwartz and others, 1998; Hall and others, 1999). At Point Arena, Prentice (1989) estimates a slip rate of ≤25 ± 2.5 mm/yr and a preferred rate of 23 ± 3 mm/yr for the past 2350-2700 years based on offset of a buried channel. Niemi and Hall (1992) conclude that the slip rate at the Vedanta site near Olema is 24 ± 3 mm/yr for the past 1800 ± 78 years. Trenches at the Filoli site on the San Francisco Peninsula exposed an offset paleochannel that yields a slip rate of 17 ± 4 mm/yr for the past 2000 years (Hall and others, 1999). WGNCEP 96 used the Point Arena and Olema results to estimate a slip rate of 24 ± 3 mm/yr for the San Andreas north of the Golden Gate and used the Filoli results of 17 ± 4 mm/yr for the SAP slip rate south of the Golden Gate. WG99 uses the 24 ± 3 mm/yr slip rate for the SAO and SAN segments and uses the17±4 mm/yr slip rate for the SAP segment and also for the SAS segment, for which there is no measured geologic rate. In the Santa Cruz Mountains, active deformation occurs across a broad volume of crust adjacent to the San Andreas fault, as indicated by the Loma Prieta rupture and the Sargent fault. The partitioning of slip onto these faults could reduce the long-term rate of the SAS.

Previous Earthquakes: Recurrence and Slip per Event

Prentice (1989) found evidence near Pt. Arena for at least five surface-faulting earthquakes during the past 2000 years. Although the dating of individual earthquakes was poorly constrained, Prentice (1989) concludes that the recurrence of ruptures along this part of the fault range from 188 to 340 years, averaging about 260 years. At the Vedanta site, Niemi (1992) and Niemi and Hall (1992) identify two pre-1906 surface faulting earthquakes in trenches across marsh deposits. The third event back was estimated to have occurred between AD 1276 and 1450; the penultimate event occurred after AD 1427-1629. In more recent work at Vedanta, Niemi and others (2002) have identified the occurrence of a least seven surface rupturing events during the past 2000 to 2500 years. Of these, at least four have occurred since 850 AD, and three

since 1250 AD, suggesting average recurrences of about 300 years for earthquakes rupturing this SAN location. South of the Santa Cruz mountains at Arano Flat, preliminary analysis of offset fluvial deposits suggests as many as six surface-rupturing events since ~1100 AD (Fumal and others, 1999). This implies a recurrence interval shorter that than the North Coast and may reflect higher activity near the transition between the locked and creeping section of the fault.

Schwartz and others (1998) compared dates of the penultimate earthquake(s) at sites along the 1906 rupture north of San Francisco and in the Santa Cruz mountains. They concluded that the similarity of ages indicated the San Andreas fault may have failed either as a sequence of closely timed earthquakes on adjacent segments or as a single long rupture similar to the 1906 earthquake near the mid 1600s, the latter interpretation being preferred. They estimated the penultimate event dates to AD 1600 to 1670, yielding an interval of 235 to 300 years between it and the 1906 earthquake, although a narrower range of AD 1630 to 1660 was also permitted by the radiocarbon dating. At Bolinas Lagoon and Bodega Harbor on SAN, Knudsen and others (2001) found buried peats at two levels. In view of the coseismic subsidence that occurred at Bolinas in 1906, Knudsen and others (2001) interpret their buried peats as an expression of coseismic subsidence from earlier events. Dating of the lower peat indicates subsidence between AD 1290 and 1340. If this dates a large earthquake, the interval between it and the penultimate event on the SAN is 260 to 380 years. The date of the older submerged peat at Bolinas lagoon is similar to the third event back at Vedanta and consistent with preliminary dates for an event at Arano flat near Watsonville (Fumal and others, 1999). While the uncertainties are considerable, these data together are consistent with the occurrence of a long rupture, similar to 1906, in the early 1300s. Overall, the paleoseismic observations indicate recurrence intervals for large earthquakes on the San Andreas fault, and particularly on SAN, to be several hundred years (ranging from 180 to 370 years).

Slip per event is diagnostic of rupture length of past earthquakes; large-earthquake slip is associated with long earthquake ruptures. Unfortunately, along the 470 km length of the 1906 rupture, only one location has been found where paleoseismic slip has been measured. At Pt. Arena, Baldwin and others (2001) found a paleochannel margin offset 4 m during the penultimate event, which is comparable to the 4.9 m measured near the site in 1906. This paleoseismic evidence for repeating long ruptures, of which the 1906 earthquake is just the most recent example, has played an important role in the source- characterization group's decisions regarding long-term rupture models of the San Andreas fault.

Rupture Sources and Scenarios

For the four-segment representation of the San Andreas fault, there are ten rupture sources and nine possible rupture scenarios, including the floating-earthquake scenario. The rupture scenarios are illustrated in **Figure 3.4.**

(1) SAO+SAN+SAP+SAS: This scenario provides for simultaneous rupture of all four segments, our 1906 facsimile earthquake rupture. A similar may have occurred in the early to mid 1600s (Schwartz and others, 1998) and in the early 1300s (Knudsen and others, 1999).

(2) SAO+SAN, SAP+SAS: This is a two source scenario with a segmentation point at the Golden Gate. Toppozada and Borchardt (1998) interpret the 1838 earthquake as a combined SAP + SAS rupture.

(3) SAO+SAN, SAP, SAS: This scenario treats the two northern segments as one and the two southern segments as separate earthquake sources. Bakun (1999) interprets the 1838 earthquake as confined to the SAP.

(3A) SAO+SAN+SAP, SAS: This scenario has the three northern segments rupturing as one, almost but not quite the 1906 earthquake facsimile (Scenario (1)), and the southern segment as an independent source.

(4) SAO, SAN, SAP, SAS: This scenario represents independent rupture of each segment.

(4A) SAO, SAN, SAP+SAS: This scenario permits independent rupture of the two northern segments and simultaneous rupture of the two southern segments.

(4B) SAO, SAN+SAP, SAS: This scenario provides for independent rupture of the northern and southern segments and simultaneous rupture of the two middle segments..

(4C) SAO, SAN+SAP+SAS: This scenario has the northern segment rupturing by itself, with the other three segments rupturing together.

(5) Floating **M** = 6.9 earthquakes: This scenario provides for strain release to be achieved by randomly placed floating earthquakes. The historical record indicates M 7 earthquakes near or along various segments of the northern San Andreas fault in 1838 (M 6.8), 1898 (M 6.8), and 1989 (M 6.9). The magnitudes of these events are the basis for the M of the floating earthquake used here.

Fault Rupture Models

The rupture scenarios presented above form a set of the possible ways in which the San Andreas fault can rupture in the course of an earthquake cycle, given our four-segment/floating earthquake representation of it. No one scenario is likely to be the only way the San Andreas fault works. The San Andreas SCG combined these rupture scenarios in different ways to define, in the end, five fault-rupture models that represents its best collective judgment about the alternative ways in which the fault can rupture in earthquakes. These models (A to E) are presented as columns in **Table 3.2**, with the nine rupture scenarios appearing as rows. Models are defined by the *scenario* weights entered as elements of the matrix. The *model* weights are given at the bottom of **Table 3.2.**

What is apparent from **Table 3.2** is that the San Andreas SCG is that four of the models (excepting model D) contain a high percentage of scenario 1. The strong preference for scenario 1 reflects the consensus view of SA/SA SCG that the fundamental behavior of the San Andreas fault is expressed as full-length, 1906-type earthquakes, which is suggested by both the historical and paleoseismic records. Scenarios 2 and 3 have in common the Golden Gate segmentation point's being a significant feature of the mechanics of the San Andreas fault. It defines the

intersection of the San Gregorio and San Andreas faults and is the locus of the slip-velocity change along the San Andreas fault. The only difference between these two scenarios is whether the southern two segments SAP and SAS rupture in unison or separately, with San Andreas SCG opinion favoring the former interpretation in the model weightings by more than 2:1. Toppozada and Borchardt (1998) interpret the 1838 earthquake as rupturing both SAP and SAS, but Bakun (1999) does not. Neither does the paleoseismic evidence at Grizzly Flat (Schwartz et al, 1998) show evidence of rupture of the 1838 earthquake through the Santa Cruz Mountains. Finally, the floating-earthquake scenario reflects SCG opinion, based on the historical seismic record, that considerable opportunity exists for the occurrence of **M** = 6.9 earthquakes without regard to the four-segment characterization of the San Andreas fault.

As discussed later, these fault-rupture models and the weighting applied to them by the San Andreas SCG will lead to a relatively large number of large magnitude events (**M** ≥ 7.5) on the San Andreas fault, given the mean magnitudes of earthquakes arising from SAO+SAN+SAP+SAS and SAO+SAN.

Table 3.2. San Andreas Fault Rupture Models and Weights

Rupture Scenario	Model A	Model B	Model C	Model D	Model E
1 SAO+SAN+SAP+SAS	76%	45%	56%	24%	49%
2 SAO+SAN, SAP+SAS	5%	45%	4%	36%	8%
3 SAO+SAN, SAP, SAS	14%	0%	12%	16%	4%
3_A SAO+SAN+SAP, SAS	0%	0%	8%	0%	0%
4 SAO, SAN, SAP, SAS	0%	0%	0%	0%	8%
4_A SAO, SAN, SAP+SAS	0%	0%	0%	2%	3%
4_B SAO, SAN-SAP, SAS	0%	0%	0%	0%	0%
4_C SAO, SAN+SAP+SAS	0%	0%	0%	2%	3%
5. Floating **M** = 6.9	5%	10%	20%	20%	25%
	100%	100%	100%	100%	100%
Model Weights	15%	23%	31%	8%	23%

San Gregorio Fault

The San Gregorio fault, the westernmost member of the San Andreas Fault system in SFBR, courses southeastward 175 km from the Golden Gate segmentation point along the western edge of the San Francisco Peninsula into and through Monterey Bay (**Figure 3.1**). Much of the San

Gregorio fault is offshore; all of the southern segment (SGS) is offshore and more than one active trace is believed to exist beneath Monterey Bay. The behavior of the San Gregorio fault is known only from its northern segment (SGN) along the San Mateo County coast where paleoseismic investigations show the occurrence of large slip events (Simpson and others, 1998). Although the most recent large-slip earthquake probably predates the historical era, there is a small probability that the 1838 earthquake occurred on SGN (Bakun,1999).

Segmentation

SA/SG SCG identified two major segments of the San Gregorio fault, the northern (SGN) and southern (SGS) segments (**Figure 3.1**).

SGN. SGN is approximately 110 km in length. It is exposed on land at only two places, between Seal Cove and Half moon Bay and at Pt. Ano Nuevo. Its northern boundary is near the Golden Gate **(Figure 3.3).** Jachens and Zoback (1999) interpret high-resolution aeromagnetic data to indicate a right-stepping en-echelon pattern of faulting for the San Gregorio fault as it appears to merge with the San Andreas fault across a 4-km-wide zone south of Bolinas Lagoon. The southern segment boundary is placed in the central part of Monterey Bay. This ~20-km long zone is co-located with the intersection of southeast-splaying, Pleistocene and Holocene oblique right-lateral and thrust faults observed from seafloor observations (D. Stakes, personal communication, 1999) and on shore south of Monterey Bay (Rosenberg and Clark, 1994). Northern Monterey Bay is also marked by a cluster of seismicity, (McNally and Stakes, 1998; Ross and *others,* 1998), as well as two **M** = 6 .1 earthquakes in 1926.

SGS. The southern boundary of the ~66-km-long SGS is located 20 km south of Pt. Sur,with an uncertainty of ±10 km **(Figure 3.5).** Geologic mapping suggests a distributed zone of shear on several faults south of Pt. Sur but no clear geomorphic connection between the San Gregorio fault and the San Simeon-Hosgri fault system 75 km to the southeast. The southern boundary adopted here coincides with WGNCEP 96's and Peterson and others (1996) south endpoint of the San Gregorio fault.

Slip Rate

Holocene slip rates on the San Gregorio fault have been difficult to obtain due to the relatively short on-land strands available for study. Multiple faulot strands increase the difficulty of obtaining full rates across the entire fault zone. WGNCEP 96 assumed a slip rate of 5 ± 2 mm/yr for SGN based on preliminary paleoseismic rates at Seal Cove and Pt. Año Nuevo. It also developed a rate of 3 ± 1.5 mm/yr for SGS, basing this largely on possible continuity with the San Simeon-Hosgri fault system and accounting for partitioning of minor slip onto structures such as the Monterey Bay-Tularcitos fault fault onshore south of Monterey Bay. WGNCEP 96 noted that these estimates were poorly constrained.

Mapping and trenching of a San Vicente Creek paleochannel offset 300-360 m at Seal Cove suggests a slip rate of 3.5 mm/yr to 4.5 mm/yr over the past 80,000-85,000 years for the eastern trace of the fault (the Seal Cove strand) (Simpson and others, 1998). This slip rate is a minimum estimate because there is an unknown amount of slip on the offshore western strand of the San Gregorio fault zone, well expressed topographically on the seafloor. Farther south, Weber and Cotton (1981), Weber (1994), and Weber and others (1997) have reported slip rates of 4-11

mm/yr across the entire zone at Pt. Año Nuevo. These rates are based on cumulative right-lateral offset of marine shoreline angles across the Coastways, Frijoles and related faults and also on right-lateral offsets of Año Nuevo Creek and Cascade Creek, as averaged over the past ~100,000 years. There are no late-Holocene slip rates available. A possible constraint on the late-Holocene rate is derived from the change in the San Andreas slip rate north and south of the Golden Gate, where the San Gregorio fault intersects the San Andreas. Here, the San Andreas slip rate decreases from 24 to 17 mm/yr. This 7 mm/yr slip-rate difference does not appear to be transmitted eastward to the Hayward fault and is likely partitioned onto the San Gregorio fault. From these observations, the San Andreas SCG adopted a slip rate for SGN of 7 ± 3 mm/yr.

The slip rate for SGS is even more problematic because no part of the fault is exposed on shore. On the southern shores of Monterey Bay, the Monterey Bay - Tularcitos - Navy - Chupines (MBNTC) fault system forms a broad zone of deformation that may carry some SGS slip to the southeast. Simila and others (1998) concluded that the two M_L 6.1 earthquakes in 1926 were located on the MBNTC fault system. However, slip rates on individual faults are not well constrained. Vaughn and others (1991) report that a segment of the Chupines fault is associated with dextrally deflected drainages and may have a slip rate as high as 2 mm/yr. If correct, this would be a minimum rate for the MBNTC zone, reducing the 7 mm/yr SGN slip rate to less than 5 mm/yr on SGS. At this time, there are no new data that warrant a change from the WGNCEP 96 report. Aware that some slip is being transferred onshore and that the slip rate on the San Simeon-Hosgri fault system may reflect that of the San Gregorio, the San Andreas SCG assigned SGN a slip rate of 3 ± 2 mm/yr.

Previous Earthquakes: Recurrence and Slip per Event

Paleoseismic data are sparse for the San Gregorio fault because of limited on-land exposure. Trench excavations at Seal Cove (Simpson and others, 1998) exposed evidence of the past two surface-faulting earthquakes. The most recent event occurred after the deposition of a native Californian cooking hearth dated AD 1270-1400 but before the arrival of the Spanish missionaries in 1776. The penultimate event at the Seal Cove site occurred between AD 620 and 1400. Given the dating uncertainties, intervals between these events could have been 300 to 690 years. Thornburg and Weber (1998) found evidence for three or four events in deposits interpreted to be as old as 6000-8000 years on the Frijoles fault strand at Cascade Ranch, near Pt. Año Nuevo, ,indicating a minimum recurrence interval of 1500-2000 years. No comparable data exist for the Coastways fault strand, although Weber, Nolan and Zinn (1993) report evidence of Holocene right-lateral slip on the Coastways fault strand.

Individual events on the San Gregorio fault appear to be large. Based on reconstruction of trench stratigraphy, Simpson and others (1998) estimated lateral slip of 5 (-2, +6) m for the most recent event and 3 (±0.2) m for the penultimate event at Seal Cove.

Rupture Sources and Scenarios

For the two-segment representation of the San Gregorio fault, there are three rupture sources, and three rupture scenarios, including the floating-earthquake (**M** = 6.9) scenario, presented below and illustrated in **Figure 3.6**:

(1) SGN, SGS: Independent rupture of both segments.

(2) SGN+SGS: Simultaneous slip of both segments.

(3) Floating **M** = 6.9 earthquakes: Given the large uncertainties about San Gregorio segmentation, the San Andreas SCG also permitted a **M** = 6.9 event to occur anywhere along the fault. The magnitude assigned to the floating source is the same as for the San Andreas fault.

SA/SG SCG also considered, and rejected, the possibility that the San Gregorio fault might rupture together with the two northern segments of the San Andreas fault (SAN and SAO) in a single large **M** ~8 event, because there was no evidence supporting this scenario.

Fault Rupture Models

All that is known about large earthquakes on the San Gregorio fault is that such events have occurred on the Seal Cove strand of SGN. Without other paleoseismic data, it is difficult to assign meaningful differences in the relative frequencies of occurrence of the rupture scenarios. As such, the San Andreas SCG defined three rupture models that cover this broad uncertainty and weighted them equally (Table 3.3).

Table 3.3 San Gregorio Fault Rupture Models and Weights

	Rupture Scenario	Model A	Model B	Model C
1	SGN, SGS	70%	35%	0%
2	SGN+SGS	0%	35%	70%
3	Floating **M** = 6.9	30%	30%	30%
	Model Weights	33.3%	33.3 %	33.3%

Hayward-Rodgers Creek Fault

The Hayward-Rodgers Creek fault system is 140 km long, extending from near Healdsburg on the north to the Warm Springs district of Fremont on the south (**Figure 3.7**). South of San Pablo Bay, the fault passes through areas heavily urbanized area where much evidence of the fault is obscured. The southern part of the fault produced the regionally damaging 1868 M 6.8 earthquake. The East Bay SCG considers the Hayward-Rodgers Creek fault to be a three-segment system, as did WG90 and WGNCEP96; significant new information is available to this study, however, which has led to some changes in the details. The discussions and conclusions of the East Bay SCG presented below have been summarized by Lettis (2001).

Segmentation

In the WG 90 and WGNCEP 96 reports, this fault system was characterized with the southern Hayward, northern Hayward, and Rodgers Creek segments. The bases for this division were differences in both timing of the most recent earthquake along the fault and major changes in fault geometry and structure along the strike of the fault. The timing differences are: 1) the occurrence of the 1868 earthquake on the southern Hayward fault; 2) the belief that a large

earthquake occurred on the northern Hayward fault in 1836 (WG90); and 3) the historical seismic record, which indicated no large magnitude earthquakes on the Rodgers Creek fault since at leas the early 1800s. The 6-km-wide releasing stepover between the Hayward and Rodgers Creek faults beneath San Pablo Bay was considered wide a stepover for ruptures to propagate through, and an additional reason to separate the northern Hayward fault from the Rodgers Creek fault.

As in the earlier reports, the East Bay SCG defines three segments for the Hayward-Rodgers Creek fault: the south Hayward (HS), north Hayward (HN), and Rodgers Creek (RC) segments (**Figure 3.7)**. The East Bay SCG considered the following important new information: a) relocation of the 1836 earthquake from the Hayward fault to south of San Francisco Bay (Toppozada and Borchardt, 1998; Bakun, 1999); b) paleoseismic data showing that the most recent large event (MRE) on the HN occurred between 1640-1776 (HFWG, 1999)and the MRE on the RC occurred between 1670-1776 (Hecker, written communication, 1999; Schwartz and others, 2001)); and c) an increase in the estimated length of the 1868 rupture using geodetic data (Yu and Segall, 1997). This new information removed a major timing constraint on segmentation relied on in previous working group reports.

RC. The Rodgers Creek fault segment is essentially unchanged from the WG90 characterization. The northern boundary is a ±5 km-wide zone south of Healdsburg in which the Holocene trace of the fault appears to die out (Hart, 1992). The southern boundary is a ±5 km zone offshore beneath San Pablo Bay. The 6 km stepover from the RC to the HN is coincident the western edge of a prominent gravity low that extends approximately 20 km to the east of the step-over. There are no geophysical data that indicate the presence of a structural depression or extensional faulting within the stepover. It is also not known whether RC and HN join at depth beneath this structure or remain individual faults through the seismogenic crust. Based on modeling of rupture propagation across steps in faults (Harris, 1995), the San Pablo Bay stepover continues to be viewed as a major structural and geometric barrier for ruptures propagating into it. That is, the SCG viewed the San Pablo Bay stepover as a particularly strong segmentation point.

HN. This northern segment of the Hayward fault extends from the San Pablo Bay stepover to near Montclair in Oakland. With the timing constraint of the most recent event (formerly the 1836 earthquake) removed, the primary basis for defining HN is that it is the section of the Hayward fault that did not rupture in 1868. An uncertainty of ±5 km is assigned to the northern boundary in San Pablo Bay. The southern endpoint is less certain. The possible north end of the 1868 rupture near Rocky Mound (Yu and Segall, 1997) is 20 km north of the segment boundary near San Leandro adopted by WG 90, where the evidence for 1868 surface rupture was distinct (Lawson, 1908). Trenching evidence suggests the 1868 surface rupture extended at least to Montclair (Lienkaemper and Williams, 1999). There are no obvious geometric or lithologic changes along this reach of the fault that provide a physical basis for proposing a segment boundary. Therefore, a southern endpoint is possible anywhere between Mira Vista on the north, which did not rupture at the surface in 1868 (HFWG, 1998) and San Leandro. The segment endpoint selected by the East Bay SCG lies at Montclair, about midway between Mira Vista and San Leandro, with an uncertainty of ± 10 km. This new endpoint shortens the HN length considerably from that used in the WG88 and WG90 reports.

HS. The East Bay SCG takes HS to be the extent of the 1868 rupture. Nothing is known about the slip distribution of the 1868 earthquake or of the variability in rupture lengths and/or slip distributions of pre-historic HS events. It is it possible that HN and HS ruptures could overlap10 to 20 km in the broad boundary between the two segments. The southern endpoint of HS is midway between the south end of known 1868 surface rupture at Agua Caliente Creek (Lawson, 1908) and the Alum Rock seismicity trend. Uncertainty in the location of this boundary is ±10 km.

Slip Rate

Slip rates for the Hayward-Rodgers Creek fault have not changed since the WG90 report. WG90 used a rate of 9 ± 2 mm/yr for each of the three fault segments based on paleoseismic and fault-creep data. WGNCEP 96 also used these rates, consistent with new paleoseismic observations of a minimum rate of 7-10 mm/yr for the past 8,400 years on HS at Union City (Lienkaemper and Borchardt, 1996) and 8.4±2 mm/yr for the past 900 years on RC (Schwartz and others, 1992). Measurements of surface creep (Lienkaemper and others, 2001) show that the Hayward fault has an average creep rate of about 4 to 6 mm/yr with a high of 9 mm/yr near Fremont, a significant fraction of the overall geologic slip rate. Williams (1999) reports a long-term (35 ka) slip rate of 10 ± 1 mm/yr on HN from offset of Strawberry Canyon. The East Bay SCG continues the use of 9 ± 2 mm/yr for HS, HN, and RC.

Previous Earthquakes: Recurrence and Slip per Event.

On the RC segment, trenching at the Triangle G site indicates the most recent surface faulting earthquake occurred after AD 1640 and before 1776 (Hecker, written communication; Schwartz et al, 2001)). At least two other events have occurred during the past 1100 years at this location, and individual recurrence intervals range from 235 to 387 years (Schwartz et al, 1992). From an offset channel at the nearby Beebe Ranch, Budding et al (1990) have estimated slip for the most recent event (MRE) event to be 2.0 (+0.3, -0.2) m. Total slip for the past three events is 5.1 to 7.2m, giving an average slip of 1.9 (+0.4, -0.3) m for these paleoearthquakes. The trench-based recurrence intervals have large uncertainties but, along with the mean calculated RI of 230 years dervived from the slip rate and slip per event, suggest intervals of 200-300 years for large surface ruptures.

At the Mira Vista site on HN, the MRE is bracketed between AD 1640 and 1776. The trenches reveal that a minimum of four to seven surface-faulting events have occurred during the past 1630 to 2130 years, providing maximum average recurrence intervals from 270 to 710 years (HFWG, 1998). Because the event history recorded at this site appears to be incomplete (HFWG, 1998) the actual rupture rate on the northern Hayward is likely to be shorter than the 270 to 710 year trench recurrence interval. Surface rupture associated with the 1868 earthquake is not evident at the Mira Vista site, thereby constraining the northern extent of the 1868 rupture. There are no data for HN on the amount of horizontal slip during past earthquakes.

The MRE on HS is the 1868 rupture. Paleoseismic investigations by Williams (1992) at the north end of Tule pond suggest six or seven earthquakes during the past 1500-2000 years, with an average repeat time of 150 to 250 years; timing of individual events, however, is not well constrained. At the south end of Tule pond, Lienkaemper et al (2002) find that four surface-faulting earthquakes have occurred between AD 1470 and 1868 for an average recurrence during

this period of 130 ± 40 years. The only information on the amount of slip during past earthquakes is the average geodetic offset of1.9 m for the 1868 earthquake (Yu and Segal, 1998).

Rupture Sources and Scenarios

For the three-segment representation of the Hayward-Rodgers Creek fault, there six rupture sources and five possible rupture scenarios (**Figure 3.2),** including the floating-earthquake (**M** = 6.9), described below.

(1) RC+HN+HS: Simultaneous rupture of all three segments, extending from the northern end of the Rodgers Creek fault to the southern end of the Hayward fault. . This scenario is permitted by the overlapping dates of the most recent event on RC and HN with the penultimate event on HS.

(2) RC+HN, HS: Simultaneous rupture of the Rodgers Creek fault with HN and independent rupture of HS. In this scenario, the San Pablo Bay step-over is considered to be the nucleation point for a bilateral rupture. The overlapping dates of the most recent large earthquakes on the HN and RC, coupled with observations that the 1995 Kobe earthquake nucleated in a 4-km-wide extensional step and ruptured bilaterally, provide the basis for the this RC+NH source in this scenario.

(3) RC, HN+HS: Independent rupture of the Rodgers Creek fault and simultaneous rupture of the two Hayward fault segments. In this scenario the San Pablo Bay step-over is a strong barrier to rupture and the HS/HN segmentation point is not a barrier to through-going rupture. The combined HN+HS source reflects the absence of a well-defined geometric or dynamic segmentation point along the Hayward fault plus the observation that rupture in 1868 occurred along more than 60 percent of the mapped surface trace of the Hayward fault.

(4) RC, HN, HS: Independent rupture of all three fault segments. The San Pablo Bay step-over plus the division of the Hayward fault into two segments based on partial rupture in 1868 form the basis for this scenario.

(5) Floating **M** = 6.9 earthquakes. This scenario allows the fault to fail in **M** = 6.9 (σ = 0.12) events that are spatially unconstrained along the length of the fault. The size of the floating earthquake is close to the magnitude estimated for the 1868 earthquake.

Fault Rupture Models

The fault rupture models considered by the East Bay SCG for the Hayward-Rodgers Creek fault are shown in **Table 3.4**, A to D. The models are quite similar, with a relatively small range in model weights. This reflects, in part, the relatively large amount of information available for the fault, which results in a narrowing of the differences that are proposed for alternative rupture models. EBay SCG has placed considerable weight on rupture scenarios 3 and 4 above in all four fault rupture models. These scenarios have RC as an independent rupture source, based on the East Bay SCG's assessment that the San Pablo Bay step-over is a strong segmentation point. The SCG gave high weights to independent rupture of all three segments (scenario 4) in each model. However, as indicated by the model weights, the East Bay SCG also favors HS and HN failing

simultaneously (models A and B), not independently, placing little confidence in the efficacy of the HS/HN segmentation point. Low weights are given to both the floating earthquake source and the rupture of the entire fault in a single event.

Table 3.4 Hayward-Rodgers Creek Fault System Rupture Models and Weights

Rupture Scenario	Model A	Model B	Model C	Model D
1 RC+HN+HS	9%	5%	7%	3%
2 RC+HN, HS	6%	10%	20%	7%
3 RC, HN+HS	55%	40%	10%	15%
4 RC, HN, HS	25%	40%	55%	70%
5 Floating **M** = 6.9	5%	5%	8%	5%
	100%	100%	100%	100%
Model Weights	22%	36%	11%	31%

Calaveras Fault

To the east of the Hayward-Rodgers Creek fault, the Calaveras fault extends 123 km, splaying from the San Andreas fault near Hollister and terminating at Danville at its northern end (**Figure 3.8**). The Calaveras fault is one of the most geologically active and complex faults in SFBR. Since the WG90 report, slip rates and recurrence estimates have been obtained at Leyden Creek, Welch Creek, and San Ysidro Creek (**Figure 3. 8)**, and monitoring of surface fault creep has continued at several localities. These data provide a better understanding of slip rates along the fault, but many questions remain about its potential to produce large earthquakes, particularly along the rapidly creeping sections south of Calaveras Reservoir. Much of the discussion of the East Bay SCG with respect to the Calaveras fault is summarized by Kelson (2002).

Segmentation

Previous studies have divided the fault into two segments based on their seismic behavior: (1) a southern segment extending from south of Hollister to Calaveras Reservoir (Bakun, 1980; Oppenheimer et al., 1990) and (2) a northern segment extending from Calaveras Reservoir to near the town of Danville (WGNCEP, 1996). Kelson *et al.* (1998) further divided the southern segment into a central segment from San Felipe Lake to Calaveras Reservoir and a southern segment from the Paicines fault south of Hollister to San Felipe Lake. The East Bay SCG adopted the three-segment model for the Calaveras fault of Kelson *et al.* (1998): northern CN, central CC, and southern CS segments (**Figure 3.8**).

CN. This segment extends 45 ± 5 km from Calaveras reservoir to Danville, the northernmost extent of identifiable Holocene faulting. An uncertainty of ±5 km allows for the possibility that ruptures terminate at structures defined by either the 1970 Danville or 1990 Alamo earthquake swarms. The south end of CN is placed at the south end of Calaveras Reservoir, which occupies a 7-km-long releasing stepover associated with a 15° change in strike of the fault. An uncertainty of ±5 km for this boundary captures the entire stepover. This southern boundry of CN also coincides with the complex, poorly understood zone of intersection of the Calaveras and Hayward faults.

The absence of microseismicity on CN (Ellsworth and others, 1982; Oppenheimer and Lindh, 1992; Oppenheimer and MacGregor-Scott, 1992), negligible to low amounts of fault creep, a lower geologic slip rate, and clear evidence of large paleoseismic surface offsets distinguish CN from CC and CS. There is evidence for only one historical earthquake on CN, the 1861 **M** = 5.8 San Ramon Valley earthquake, for which Jennings (1994) shows a 4-km-long rupture on the Calaveras fault. However, it is uncertain whether this was a coseismic surface rupture or shaking induced. Creep rates are significantly lower along CN than they are to the south. The historical creep rate on CN in the Pleasanton-Sunol area is 2.5 to 3.5 mm/yr (Mosier, 1977; Prescott *et al.*, 1981; Burford and Sharp, 1982; Prescott and Lisowski, 1983). Farther north in San Ramon, Galehouse and Lienkaemper (2002, BSSA) and colleagues measured a rate of 1.7 mm/yr between 1981 and 1999. This contrasts with creep rates of 6 mm/yr at Calaveras reservoir (Prescott *et al.*, 1981) and rates as high as 13.5-16.3 mm/yr on CS at Coyote Ranch (Galehouse and Lienkaemper, 2002). Paleoseismic investigations just north of Calaveras Reservoir at Leyden Creek and Welch Creek sites (**Figure 3.8**)) provide Holocene slip rates of 5 (+2, -1) mm/yr (Kelson *et al.*, 1996) and 6 ± 1 mm/yr (Simpson *et al.*, 1999), respectively. This contrasts with a rate of 14 ± 5 mm/yr for the past 4000 years (Kelson and others, 1998) on CC at San Ysidro Creek. In addition, the Leyden Creek and Welch Creek sites provide evidence, distinct from creep, for the occurrence of surface-faulting earthquakes.

CC. This segment extends 59 ± 10 km from Calaveras Reservoir to San Felipe Lake to Calaveras Reservoir where the fault strike changes 7°. The location uncertainty associated with the south boundary is assigned a value of ±5 km to include the possibility of a rupture extending to the intersection between the Calaveras and the Busch Ranch faults 4 km south of San Felipe Lake. San Felipe Lake also marks the south end of the 1979 Coyote Creek earthquake rupture at depth.

CC is characterized by abundant microseismicity (Bakun, 1980, 1984; Bakun and others, 1986: 1985; Oppenheimer *et al.*, 1990), which may reflect the high rate of creep. The simple average creep rate from 1968 to 1999 is 16.3 mm/yr (Galehouse and Lienkaemper, 2002), although this value includes slip possibly triggered by the 1989 Loma Prieta earthquake (Galehouse, 1997). At a site about 5 km southeast of the Coyote Ranch array, Kelson *et al.* (1998) obtain an average slip rate of 14 ± 5 mm/yr since the middle Holocene. Within the uncertainty of the geologic data, the long-term slip rate on the central Calaveras is consistent with the short-term slip rate derived from aseismic slip data and geodetic modeling.

In addition to abundant microseismicity, CC has also been the source of moderate-magnitude earthquakes (1949 Gilroy, M_L 5.2; 1979 Coyote Lake, M 5.9; 1984 Morgan Hill, M 6.2; 1988

Alum Rock, M 5.1). A similar sequence of comparably-sized earthquakes occurred between 1897 and 1911. Recent syntheses characterize the central Calaveras fault as capable of producing earthquakes no larger than M 6.2 (Peterson *et al.*, 1996; WGNCEP, 1996). Agreement between the geodetic/creep rates and the geologic slip-rates (Kelson and others, 1992a) suggests that there is little or no strain accumulation along the fault that would result in a large earthquake. Based on these relations, the WGNCEP (1996) assumed that the 1984 Morgan Hill earthquake (M 6.2) is the maximum magnitude event to occur on the central Calaveras fault and calculated a repeat time of 60 years for an earthquake of this size. On the other hand, evidence from trenches at San Ysidro Creek can be interpreted as support for more than 2m-displacement surface-rupturing earthquakes along the central Calaveras fault, with three events occurring in the past 3 ka (Kelson *et al.*, 1998).

CS. CS extends 19 ± 5 km from the restraining bend at San Felipe Lake southward to the intersection with the Paicines fault, about 7 km south of Hollister. The southern boundary is a complex intersection, with the two faults merging in a series of subparallel fault strands, and this endpoint is assigned an uncertainty of ± 5 km. CS has experienced a low level of microseismicity from1963 to 1997 (Walters and Oppenheimer, in press).

Slip Rate

The slip rate on the Calaveras changes significantly where the Hayward fault splays northwest from it. WGNCEP 96 assigned a rate of 6±2 mm/yr to the northern Calaveras and 15 ±2 mm/yr to the southern Calaveras (CC and CS in the present report). The rates for CN were based on offsets of channel margins at Leyden Creek that yielded a slip rate of 5±2 mm/yr for the past 2300 years (Kelson et. al, 1996) and a 6mm/yr creep rate on a small-aperture geodetic net at Calaveras Reservoir (Prescott and Lisowski, 1983). Since 1996, Simpson *et al.* (1999) have developed a late-Holocene slip rate at Welch Creek of 6±2 mm/yr. The East Bay SCG thus retains the rate of 6±2 mm/yr for CN.

Creep rates used here for the new CC segment are best documented at the Coyote Ranch alignment array near Coyote Lake, which was measured intermittently by the USGS between 1968 and 1988. Measurements resumed at this site in early 1997. As of mid-May 1999, the average creep rate for 1968 to 1999 was 16.3 mm/yr (Galehouse and Lienkaemper, 2002), although this value includes slip possibly triggered by the 1989 Loma Prieta earthquake (Galehouse, 1990). Measurements made since 1997 provide an average rate of 13.5 mm/yr (J. Galehouse, written comm., 1999). Similar rates are observed at San Ysidro Creek, 5 km southeast of the Coyote Lake array, where dating of offset buried stream channels provides a preliminary geologic slip rate of 14 ± 5 mm/yr for the past 4000 years (Kelson *et al.*, 1998). With these new observations, the East Bay SCG assigns a slip rate of 15±3 mm/yr to both the CC and CS segments.

Previous Earthquakes: Recurrence and Slip per Event

There are no data to constrain well the timing of the MRE on CN. Observations at Leyden Creek (Kelson *et al.*,1996) and Welch Creek (Simpson et. al., 1999), indicate that the MRE occurred between AD 1160 and 1425. Five or six scarp-forming surface faulting events have occurred during the past 2,500 years, suggesting a geologically based recurrence interval of 550 ± 300 years (Kelson *et al.*, 1996). At the Welch Creek site in Sunol, trenching by Simpson *et al.*(1999)

allows an interpretation of three surface ruptures during approximately the same time interval. Neither of the sites yielded well-constrained timing of the MRE. No measurement of horizontal silp per event is available at either of these sites.

There is also uncertainty regarding the nature of earthquake recurrence on CC and CS. Trench exposures at San Ysidro Creek suggest that surface-rupturing earthquakes may have along CC (Kelson *et al.*,1998). They interpret offset paleochannels as evidence of large coseismic slip events on the fault and suggest a minimum of three discrete surface-rupturing earthquakes between about 4 ka and 2 ka. As such, the East Bay SCG allows the possibility of large-magnitude ruptures on CC. Although the weight of seismologic and geodetic evidence supports the interpretation that CC and CS are capable of producing only moderate-magnitude earthquakes, the geologic interpretations at San Ysidro are the reason for the East Bay SCG's including rupture models that produce large events on these rapidly creeping segments.

Rupture Sources and Scenarios

Like the Hayward- Rodgers Creek fault, the three-segment representation of the Calaveras fault has six possible rupture sources and five possible rupture scenarios. The East Bay SCG constructed the six rupture scenarios given below, using two possibilities for the floating earthquake scenario.

(1) CN+CC+CS): Simultaneous rupture of all three segments extending from Danville to Hollister.

(2) CN+CC, CS: Simultaneous rupture of the northern and central segments, and independent rupture of the southern Calaveras. Kelson and others (1996) note that the trenches at the Leyden Creek site may contain evidence for overlapping ruptures from the northern and central Calaveras segments.
(3) CN, CC+CS: Independent rupture of the northern segment and simultaneous rupture of the central and southern segments.

(4) CN, CC, CS: Independent ruptures of the three segments.

(5) CN and floating **M** = 6.2 earthquake: Independent rupture of the northern Calaveras fault coupled with floating earthquakes along the central and southern fault segments. **M** = 6.2 is the magnitude of the 1984 Morgan Hill earthquake.

(6) Floating **M =** 6.2 earthquakes: **M** = 6.2 earthquakes spatially unconstrained along the entire fault sytstem.

Fault Rupture Models

EBay SCG developed four rupture models for the Calaveras fault, with a clear preference for rupture models that have the boundary between the northern and central Calaveras as a strong segmentation point. This preference reflects the collective judgment that the changes in creep rate, slip rate, seismicity, and geometry that occur near the Calaveras reservoir express a basic change in the rupture behavior of the Calaveras fault. Uncertainties in the behavior of the rapidly creeping central and southern segments are clearly reflected in the high weighting of

models B and C. These have moderate (model C) to high (Model B) weights on scenarios that contain the floating earthquake as the dominant rupture mode; each also allows the possibility of large events. Model B, which rules out multi-segment ruptures and places high weight on an independent CN and floating earthquakes elsewhere, received the highest weighting of any of these models. While long ruptures involving multiple segments are permitted, the East Bay SCG considered these to be very infrequent events.

Table 3.5 Calaveras Fault Rupture Models and Weights

Rupture Scenario	Model A	Model B	Model C	Model D
1 CN+CC+CS	5%	0%	5%	5%
2 CN+CC, CS	5%	0%	5%	5%
3 CN, CC+CS	25%	0%	5%	5%
4 CN, CC, CS	40%	20%	40%	60%
5 CN, Floating **M** = 6.2	20%	70%	40%	15%
6 Floating **M** = 6.2	5%	10%	5%	10%
	100%	100%	100%	100%
Model Weights	10%	50%	30%	10%

Concord-Green Valley Fault System

The Concord-Green Valley fault extends from the vicinity of Walnut Creek north to Wooden Valley, a distance of approximately 56 km (**Figure 3.9**). Large earthquakes have not occurred on the Concord-Green Valley fault during the historical period, although a M**s** 5.4 earthquake occurred on the central part of the Concord fault in 1955. Aseismic slip occurs locally along sections of the Concord-Green Valley fault, with rates increasing from about 4 mm/yr for the past 18.5 years in Concord to 5 mm/yr near Cordelia (Galehouse, 1998). The deliberations of the East Bay SCG on the Concord-Green Valley fault are summarized by Borchardt and Baldwin (2001) and are discussed below.

Segmentation

WGNCEP 96 considered the Concord-Green Valley fault to consist of two segments, the Concord and Green Valley segments based on a minor (5°) change in strike of the fault beneath Suisun Bay. The East Bay SCG defines the northern Green Valley (GVN), the southern Green Valley (GVS), and the Concord (CON) segments for this fault, as described below and shown in **Figure 3.9**.

GVN. This segment is short with a length of just 14 ± 4 km. The north end is marked by an abrupt termination of the fault as a prominent geomorphic feature, although slip may be transferred northwest across a series of west-vergent folds and thrust faults (Baldwin and others, 1998). The south boundary is a minor bend or stepover to the southern Green Valley fault near the Green Valley Golf Course. An additional structural complexity occurs near this location where the Cordelia fault,which has a slip rate about 0.5 mm/yr, may branch at depth from or form a right step over from the Green Valley fault. The uncertainty in the location of the south end of the segment boundary ±5 km.

GVS. This segment extends for 22 km from the Green Valley Golf Course on the north to Suisun Bay on the south. On its south end, a 7° releasing bend occurs where the fault crosses joins the Concord segment. This bend is the largest geometric change along the fault. A small increase in the creep rate on the southern Green Valley segment is coincident with this bend (Galehouse, 2001)

CON. The southern termination of the Concord fault is mapped as several discontinuous fault strands along the base of Lime Ridge, a northwest-trending extension of the Mt. Diablo anticlinorium (Wills and Hart, 1992). This part of the fault is poorly defined geomorphically and the SCG extended it south to its intersection with the Mt. Diablo thrust fault in the southern Walnut Creek area (Unruh and Lettis, 1998).

Slip Rate

WGNCEP 96 assigned a geologic slip rate of 6 ± 2 mm/yr for the entire fault zone. The primary basis was the assumption that slip on the northern Calaveras fault (6 mm/yr) steps to the Concord fault and that creep rates as high as 8 mm/yr have been observed on this fault system north of SFBR. Given the slip rate of 3.4 ± 0.3 mm/yr over the past 6,000 years at Galindo Creek (Borchardt *et al.*, 1999), the minimum slip rate of 3.8 to 4.8 mm/yr over the past 350 years at Lopes Ranch (Baldwin and Lienkaemper, 1999), and creep rates averaging 4.9 mm/yr for the past 18 years on the Green Valley fault at Red Top Road, the East Bay SCG assigns rates of 4 ±2 mm/yr and 5 ± 3 mm/yr to the Concord and Green Valley segments, respectively.

Previous Earthquakes: Recurrence and Slip per Event

At present there is no direct information on the timing of individual earthquakes along the Concord-Green Valley fault. Trenches on the northern part of the Concord fault show discrete offsets in alluvium (Hart and Bryant, 1997) indicative of multiple episodes of surface fault rupture, although paleoearthquake dates are not available. At the the Lopes Ranch site, trenches exposed evidence of discrete surface-faulting events on the Green Valley fault during the past 2,700 years, but the number and timing of these events are poorly known.

Rupture Sources and Scenarios

For the three-segment representation of the Concord-Green Valley fault, there are six rupture sources and five possible rupture scenarios described below.

(1) CON+GVS+GVN: Simultaneous rupture of all three segments, extending from the northern end of the Green Valley fault to the southern end of the Concord fault.

(2) CON+GVS, GVN: Simultaneous rupture of the Concord fault with the southern Green Valley fault and independent rupture of the northern Green Valley fault.

(3) CON, GVS+GVN: Independent rupture of the Concord fault and simultaneous rupture of the northern and southern Green Valley segments.

(4) CON, GVS, GVN: Independent rupture of all three segments.

(5) Floating **M** = 6.2 earthquakes: Rupture of the Concord-Green Valley fault in **M** = 6.2 events spatially unconstrained along the fault. The East Bay SCG considered this **M** to be representative of moderate size events on a creeping fault.

Fault Rupture Models

Ebay SCG developed three fault rupture models that reflect a broad range of opinion and much uncertainty about the seismogenic behavior of the Concord-Green Valley fault. This uncertainty derives mainly from the lack of paleoearthquake datesto distinguish rupture segments. The highest weight is given to Model A, which acknowledges segmentation and the occurrence of moderate-to-large earthquakes, but has no preferred rupture scenario. Model B, which strongly favors rupture of the entire fault system in a single event, also received a relatively high weighting. Model C places a very high weight on the floating-earthquake scenario;the low weight for this model reflects the trench observations of repeated surface ruptures, which are commonly associated with earthquakes larger than **M** = 6.2.

Table 3.6. Concord-Green Valley Fault Rupture Models and Weights

Rupture Scenario	Model A	Model B	Model C
1 CON+GVS+GVN	20%	80%	5%
2 CON+GVS, GVN	20%	5%	5%
3 CON, GVS+GVN	20%	5%	5%
4 CON, GVS, GVN	20%	5%	5%
5 Floating **M** =6 .2	20%	5%	80%
	100%	100%	100%
Model Weights	48%	33%	19%

Greenville Fault

The Greenville fault is the easternmost strand of the San Andreas strike-slip fault system in SFBR (**Figure 3.1, Figure 3.10**). It extends from the eastern flank of Mt. Diablo south to San Antonio Valley, a length of 43 ± 20 km. The Greenville fault is the least studied and most poorly known of the strike-slip faults considered in this study. The central Greenville fault produced **M** = 5.8 and 5.4 earthquakes in 1980 (Bolt *et al.*,1981). Microseismicity displays a subvertical alignment of epicenters extending to depths of approximately 17 km at the latitude of Livermore Valley (Hill *et al.*, 1990). For the Greenville fault, WCNCEP 96 assigned a slip rate of 2 ± 1 mm/yr; a length and width of 73 km and 11 km, respectively; and a maximum earthquake of **M** = 6.9 with recurrence interval of 550 years. WGNCEP 96 did not segment the Greenville fault.

Segmentation

The segmentation proposed by the East Bay SCG, the northern Greenville (GN) and southern Greenville (GS) segments, is based largely on differences in geomorphic expression of Holocene faulting and the location of the 1980 earthquakes. WG 02 currently proposes two segments (Figure 3.11), although three were used three segments in our earlier model (WG 99). This change was made to reflect shortening of the northern extent of Holocene displacement along the Greenville fault based on re-evaluation of geologic mapping.

GN. The north segment boundary is chosen to coincide with the northern end of the aftershock zone of the 1980 **M** = 5.8 earthquake. Most of GN is geomorphically well expressed with clear evidence of Holocene activity. Minor right lateral surface offset occurred on the GN during the 1980 Livermore earthquake (Hart, 1981). The southern termination of GN is the structural intersection with the left-lateral Las Positas fault near the southern margin of the Livermore Basin. The length of GN is 27 km.

GS. GS extends southward from GN to San Antonio Valley, and is clearly identified by its geomorphic expression of Holocene fault activity, including linear valleys, deflected and beheaded drainages, and uphill-facing scarps. The southern boundary of GS is not well defined. Unruh and Sawyer (1999) suggest that the fault forms a left-restraining step-over to the Ortigalita fault across the Mt. Oso anticline. The East Bay SCG places the southern end of GS at the Mt. Oso anticline with an uncertainty of ±10 km. The length of GS is estimated at 24 km.

Slip Rate

The Greenville fault has traditionally been viewed as having a low slip rate. Wright and others (1982) estimated a late-Quaternary rate of 0.5 to 0.7 mm/yr based on 90 m of dextral offset on stream terraces during the past 125 to 180 ka. Ages of these terraces, based on soil-profile development, are highly uncertain. Paleoseismic trench investigations across one strand of the Greenville fault documented Holocene surface-rupturing events. Assuming a 1:3 ratio of vertical-to-horizontal separation, Wright and others (1982) estimated a horizontal slip rate of approximately 0.1 to 0.3 mm/yr.

Unruh and Sawyer (1997) proposed that contractional deformation in the Mt. Diablo-Livermore area is primarily the result of a restraining stepover between the Greenville and Concord faults.

If this model is correct, then the late-Cenozoic shortening rate across Mt. Diablo can be used to estimate a long-term average slip rate for the Greenville fault. Including the uncertainties in these data, the average rate of horizontal motion parallel to the Greenville fault due to shortening in the Mt. Diablo fold-and-thrust belt is about 1.4 mm/yr (7 km in 5 million years) to about 3.5 mm/yr (12 km in 3.4 million years).

EBay SCG opted for the better determined, but longer-term averaged slip rate of 2 ± 1 mm/yr on the Greenville fault to satisfy the kinematic model for growth of the Mt. Diablo anticline and related contractional structures in the Livermore area. The clear geomorphic expression of the Greenville fault does not seem consistent with slip rates of just fractions a mm/yr

Previous Earthquakes: Recurrence and Slip per Event

These data do not presently exist for either segment of the Greenville fault.

Rupture Sources and Scenarios

The two-segment representation of the Greenville fault, there are three rupture sources and three rupture scenarios, including the floating-earthquake (**M** = 6.0) scenario:

(1) GN+GS: Simultaneous rupture of both segments.

(2) GN, GS: Independent rupture of the two segments.

(3) Floating **M** = 6.2 earthquakes: The Greenville fault fails in spatially unconstrained **M** = 6.02 earthquakes, approximately the size of the larger of the1980 earthquakes.

Fault Rupture Models

In the absence of paleoseismic data, the East Bay SCG constructed the three rupture models shown in Table 3.7, weighting equally at 1/3 each.

Table 3.7. Greenville Fault Rupture Models and Weights

	Rupture Source	Model A	Model B	Model C
1	GN+GS	70%	35%	0%
2	GN, GS	0%	35%	70%
3	Floating M 6.2	30%	30%	30%
	Model Weights	33.3%	33.3 %	33.3%

Thrust and Reverse Faults

The Thrust and Reverse Fault Source Characterization Group (Thrust and Reverse SCG) met four times in 1998 to review the state of knowledge regarding thrust faults as seismic sources in SFBR. The Thrust and Reverse SCG reviewed geodetic data, geologic data, and global plate

motion models that provide constraints on rates of deformation across the boundary between the Pacific plate and the Sierra Nevada-Great Valley microplate. Considered together, these data do not support large shortening rates (> 3 to 6 mm/yr) directed at a high angle to the plate boundary. GPS data in SFBR indicate that the *maximum* rate of boundary-normal shortening is about 3-4 mm/yr. The group discussed two end-member models for accommodating boundary-normal shortening: (1) the shortening may be uniformly distributed among many structures across the entire plate boundary; or (2) the shortening may be accommodated by a single fault or localized within a discrete contractional domain (e.g., the "Coast Range-Sierra Block boundary zone"). In the former case, it is unlikely that any single thrust fault would have a slip rate in excess of 1 to 2 mm/yr. In the latter case, we would expect to observe geologic, seismic and geodetic evidence for locally high contractional strain rates; i.e. a contractional "hot spot". It was also noted that contractional "hot spots" may be associated with restraining geometries of strike-slip faults, where local contractional strain rates are more directly related to the slip rate on the specific strike-slip fault than a component of boundary-normal shortening.

Following the assessment of regional shortening rates in the Bay Area, the group developed the following list of potential "hot spots" where significant contractional deformation may be occurring:

1) Northeastern Santa Cruz Mountains
2) East Bay Hills
3) Mt. Diablo-Livermore Region
4) Sacramento-San Joaquin Delta
5) Coast Ranges-Sierra Block Boundary Zone
6) Howell Mountains
7) Miyacamas Mountains
8) Northern SFBR (Marin, Bodega)
9) Mare Island

Specific thrust-fault sources, or evidence for distributed late-Cenozoic contractional deformation within an areal source zone, were discussed for each of these areas. These discussions, summarized by Unruh (2001), singled out the Mt. Diablo thrust as having a slip rate >1 mm/yr. On this basis it was included as an SFBR earthquake source.

Mt. Diablo blind thrust fault

The Mt. Diablo thrust is a blind thrust fault, one not observable at the Earth's surface **(Figure 3.1, Figure3.10)**. The fault itself, its geometry, and rates of slip are inferred from structural and kinematic models of Mt. Diablo. Mt. Diablo is an antiicline associated with a belt of late-Cenozoic folds and thrust faults (the "Mt. Diablo fold-and-thrust belt" of Crane (1995) and Unruh and Sawyer (1997)) that can be traced continuously for 70 km from the northern Diablo Range to the western Sacramento–San Joaquin Delta. Compressional structures within this belt are oriented WNW–ESE; exhibit a well-defined, right-stepping, en-echelon pattern; and are bounded by the Greenville fault to the southeast and the Concord fault to the northwest. Crustal shortening within this belt appears to be driven a restraining transfer of slip from the Greenville fault to the Concord fault (Unruh and Sawyer, 1997). The Mt. Diablo thrust fault is thought to

underlie the asymmetric, southwest-vergent Mt. Diablo and Tassajara anticlines for a total length of 25 ± 5 km (Crane, 1995; Unruh and Sawyer, 1997).

Considerable debate surrounded the inclusion of the Mt. Diablo thrust as an SFBR source because it is an inferred structure. Even so, this fault is required to explain the structure, topography, and youthful tectonic geomorphology of Mt. Diablo. In its review of Bay Area contractional structures, the Thrust and Reverse SCG identified the Mt. Diablo thrust as the reverse fault with the highest slip rate in SFBR, 3 ± 2 mm/yr. The geometry of the fault and its potential rupture area are estimated from balanced cross-sections, as well as comparisons of the dimensions of the Mt. Diablo anticline to folds overlying the 1983 Coalinga and 1994 Northridge earthquakes (Unruh and Sawyer, 1997). The subsurface rupture length and its uncertainty are shown in **Figure 3.11**. There is no basis for segmenting the fault, and it is treated as a single earthquake source. Geometric relations between the Mt. Diablo thrust and the Greenville fault suggest that the Mt. Diablo thrust is truncated by the Greenville fault.

Slip Rate

Available slip-rate estimates for the Mt. Diablo thrust fault are long-term average rates derived from balanced cross-sections and analysis of stratigraphic relations to determine when shortening began.

For the range of values in horizontal shortening, fault-dip orientation, and timing of deformation summarized in Unruh and Sawyer (1997), the minimum slip rate on the Mt. Diablo thrust fault is about 1.3 mm/yr (10 km total shortening; 30° fault dip; 9 Ma onset of shortening). The maximum slip rate permitted is 7 mm/yr (17 km total shortening; 45° fault dip; 3.4 Ma onset of shortening). The SCG considered the 7 mm/yr rate to be too high: if the kinematic model of Unruh and Sawyer (1997) is correct, a slip rate of 7 mm/yr on the Mt. Diablo thrust fault would require relatively high slip rates (> 3 mm/yr) on the Greenville fault, for which there no observational support. The SCG slip-rate range for the Mt. Diablo thrust is 3 $\pm$ 2 mm/yr.

Summary of Geologic Data for Fault Segments

Segment Lengths

Fault segment length is calculated from the segment endpoints identified for each fault segment. Each segment endpoint is represented by three weighted options, a preferred location and two bounding locations. These represent ~90% confidence bounds on endpoint position. The length of each segment is calculated as the along-strike distance between its endpoints (**Figure 1.3**), accounting for any internal bends. Given three positions of each endpoint, a fault segment may have up to nine possible lengths. The preferred (median) length computed from the preferred endpoint positions and the minimum and maximum lengths are listed in **Table 3.8**.

Segment Widths

Fault width refers to the down-dip depth range over which seismic faulting is possible. Widths are determined by the distribution of regional seismicity and heat flow data, with the depths of microearthquakes being the primary consideration. The base of the seismogenic zone is defined by the depth extent of small-magnitude seismicity associated with each fault, which varies across

SFBR; heat flow data and models were also used to constrain fault width (**Appendix A**). The fault-parallel seismicity cross-sections used in these estimates are shown in **Figure 3.12**. The average depth of seismicity in SFBR is 11-12 km, although locally it extends to 14-16 km. The areas of deepest seismicity, which include the Santa Cruz Mountains and the Mt. Diablo region, are regions of transpression in the strike-slip system where crustal shortening locally thickens the brittle crust.

Seismogenic Scaling Factor, *R*

Faults that creep are common in SFBR but otherwise rare among active faults in continental crust. Aseismic slip at depth occurs *in lieu* of slip during earthquakes so that an accurate accounting of the extent and amount of aseismic slip at depth is essential. While aseismic slip is a clear surface feature of the Hayward, Calaveras, and Concord–Green Valley faults, its depth extent and role in seismogenesis is poorly understood. Creep can be viewed as a vehicle for reducing the rate of strain accumulation (effectively reducing the slip rate accounted for in earthquake slip), or for reducing the fault area over which seismic slip occurs (or some combination of the two). In this analysis, fault creep is accommodated by reduction of fault area available for earthquake production.

Fault creep is represented in the SFBR earthquake model as the seismogenic scaling factor *R*, which varies from $R = 0$ (all slip occurs aseismically) to $R = 1$ (all slip occurs in earthquakes). *R* then represents the percentage of the fault plane area that is locked between coseismic events, in the same manner that Oppenheimer *et al.*, (1990) represented the central segment of the Calaveras fault. The Calculation Sequence scales the area of the fault segment that slips in earthquakes (Section 4). Thus, *R* affects the size of segment-rupturing earthquakes and thus their mean rate: the smaller the value of *R*, the smaller the seismogenic area. The smaller the area, the smaller the magnitude and seismic slip of earthquakes, and the more frequent those earthquakes must occur to balance the long-term slip rate.

An expert group convened by WG02 considered methods for constraining values of *R*. The group concluded that regional models based on geodetic observations collected in the past few decades should be the primary basis for the *R* values used in the calculations. Discussion of the appropriate models for estimating *R* for each fault segment from geodetic observations is contained in **Appendices B and C**. **Table 3.8** lists the values and weights used in the present report. The range of *R* varies from a high of 0.9–1.0 for the faults that either lack microearthquake activity that indicates creep or show no evidence of surface creep, to a low value of 0.0–0.4 for the southern Calaveras, which is creeping near or at its long-term slip rate. The Mt. Diablo thrust is assigned R=1.0 (all seismogenic) because the Working Group is unaware of documented creep on near-surface thrust faults in the Bay region and because uncertainty in the seismogenic area of this fault is incorporated into the endpoint and width values. The distribution of weights for all but the Concord-Green Valley fault and the Central Calaveras (CC) fault segment represents 90% confidence bounds. The weights for the Concord-Green Valley reflect the higher degree of uncertainty in the large-earthquake behavior this fault.

Historical seismicity and deformation data are consistent with a creeping CC segment failing in **M**6.2 earthquakes every 50-100 years. Geologic evidence suggests, however, that the CC fault segment might fail in **M**7 events every 2000 years or so. Our preliminary model results (those

adopted by WG99) were characterized by frequent **M**6.5 events, rather than frequent **M**6.2 events and infrequent **M**7 events. We found that this model mismatch could be eliminated by adjustments in *R* that did not violate available geodetic information. The Working Group voted to adopt branches with $R = 0.1$, 0.3, and 0.5 rather than the initial values of 0.3, 0.5, and 0.7.

Implications of *R* factor treatment to hazard modeling

WG02 used *R* factors to account for the effects of creep in its long-term model. As described in **Appendix B**, WG02 used *R* to reduce the seismogenic area of a fault segment, consistent with Oppenheimer et al.'s (1990) descriptions of the behavior of the creeping fault segments CC and CS. Oppenheimer et al. (1990) identified six aseismic zones at depths of about 5 to 10 kilometers as the locations of future 5< **M** <~6 earthquakes. WG02's reduction of the seismogenic area reduces the magnitude of segment-rupturing events. WG02 specifies neither the location of these reduced area events on the fault nor the distributions of slip on the areas, as this level of model detail is not relevant to estimation of earthquake recurrence rates and probabilities. However, this level of detail may be important to hazard estimates at near-fault sites where ground motions of **M**<6 events may contribute significantly to the hazard estimate. The distributions of slip during the 1979 **M**5.7 Coyote Lake and 1984 **M**6.2 Morgan Hill earthquakes on CC are illustrative of the range of source models that must be considered in hazard models. Whereas slip in the Coyote Lake event apparently was concentrated in a circular zone at 5-to-10 depth (Liu and Helmberger, 1983), slip in the Morgan Hill event was concentrated at the ends of the 15-to-20 km long rupture, with little slip near the center of the rupture length (Hartzell and Heaton, 1986). Nearly all of the strong ground motions were generated in the 1-meter slip at the end of the rupture (Bakun et al, 1984). Hazard models should encompass these examples and conform, in a statistical sense, to the distribution of nearly-constant 30-bar stress drops documented for crustal strike-slip earthquakes in numerous publications (e.g., Thatcher and Hanks, 1973; Hanks and Bakun, 2002).

Fault segment slip rate, *v*

Fault segment slip rates were estimated primarily from observations of offset geological or cultural features, and thus are average values over some time interval, typically hundreds to several tens of thousands of years. Preferred and 95%-bounding values were prescribed for each fault segment as described in this chapter. Values are summarized in **Table 3.8**.

Table 3.8 Length, width, *R* (seismogenic scaling factor), and slip rate for each fault segment

		Length, km			Width, km		R (seis. scaling factor)		Slip rate, mm/yr	
Fault	Seg.	Preferred	Min	Max	Preferred	90% bounds	Values	Weights*	Preferred	95% bounds
San Andreas	SAS	62	47	77	15	13-17	0.8/0.9/1.0	(a)	17	13-21
	SAP	85	60	110	13	11-15	0.9/1.0	(b)	17	13-21
	SAN	191	171	211	11	9-13	0.9/1.0	(b)	24	21-27
	SAO	135	115	155	11	9-13	0.9/1.0	(b)	24	21-27
Hayward/RC	HS	53	34	71	12	10-14	0.4/0.6/0.8	(a)	9	7-11
	HN	35	20	50	12	10-14	0.4/0.6/0.8	(a)	9	7-11
	RC	63	53	73	12	10-14	0.9/1.0	(b)	9	7-11
Calaveras	CS	19	9	29	11	9-13	0.0/0.2/0.4	(a)	15	12-18
	CC	59	49	69	11	9-13	0.1/0.3/0.5	(c)	15	12-18
	CN	45	35	55	13	11-15	0.7/0.8/0.9	(a)	6	4-8
Concord/GV	CON	20	12	28	16	14-18	0.2/0.5/0.8	(d)	4	2-6
	GVS	22	16	28	14	12-16	0.2/0.5/0.8	(d)	5	2-8
	GVN	14	6	22	14	12-16	0.2/0.5/0.8	(d)	5	2-8
San Gregorio	SGS	66	46	86	12	10-14	0.8/0.9/1.0	(a)	3	1-5
	SGN	110	85	134	13	11-15	0.8/0.9/1.0	(a)	7	4-10
Greenville	GS	24	15	31	15	12-18	0.8/0.9/1.0	(a)	2	1-3
	GN	27	17	37	15	12-18	0.8/0.9/1.0	(a)	2	1-3
Mt Diablo	MTD	25	15	35	14	12.2-16.2	1.0	1.0	2	1-3

* Weights: (a) Mean and 90% bounds: 0.185/0.63/0.185. (b) Only lower 90% bound set: 0.185/0.815. (c) Weights determined by WG02: 0.4/0.5/0.1 (see text). (d) Equal weighting of 1/3 on each branch.

Summary of Time of Most Recent Rupture of SFBR Fault Segments

The elapsed time since the most recent, segment-rupturing earthquake (MRE) is an important input for the time-dependent probability models, because the "segment clock" is set at this time (**Chapter 5**). The available data for the dates of large earthquakes on SFBR fault segments is summarized in **Table 3.9.** For many of these segments there is no paleoseismic information. The assumptions used to estimate the reset times on the segments for which there are no direct data, and the weights on the distribution of all reset dates, are found in **Chapter 5**.

Table 3.9. Time of most recent rupture on SFBR fault segments

Fault	Seg.	MRE date
San Andreas	SAS	1906
	SAP	1906
	SAN	1906
	SAO	1906
Hayward/Rodgers Creek	HS	1868
	HN	1635-1776
	RC	1670-1776
Calaveras	CS	No direct data
	CC	No direct data
	CN	1670-1830
Concord/Green Valley	CON	No direct data
	GVS	No direct data
	GVN	No data
San Gregorio	SGS	No direct data
	SGN	1270-1776
Greenville	GS	No direct data
	GN	No direct data
Mount Diablo Thrust	MTD	No direct data

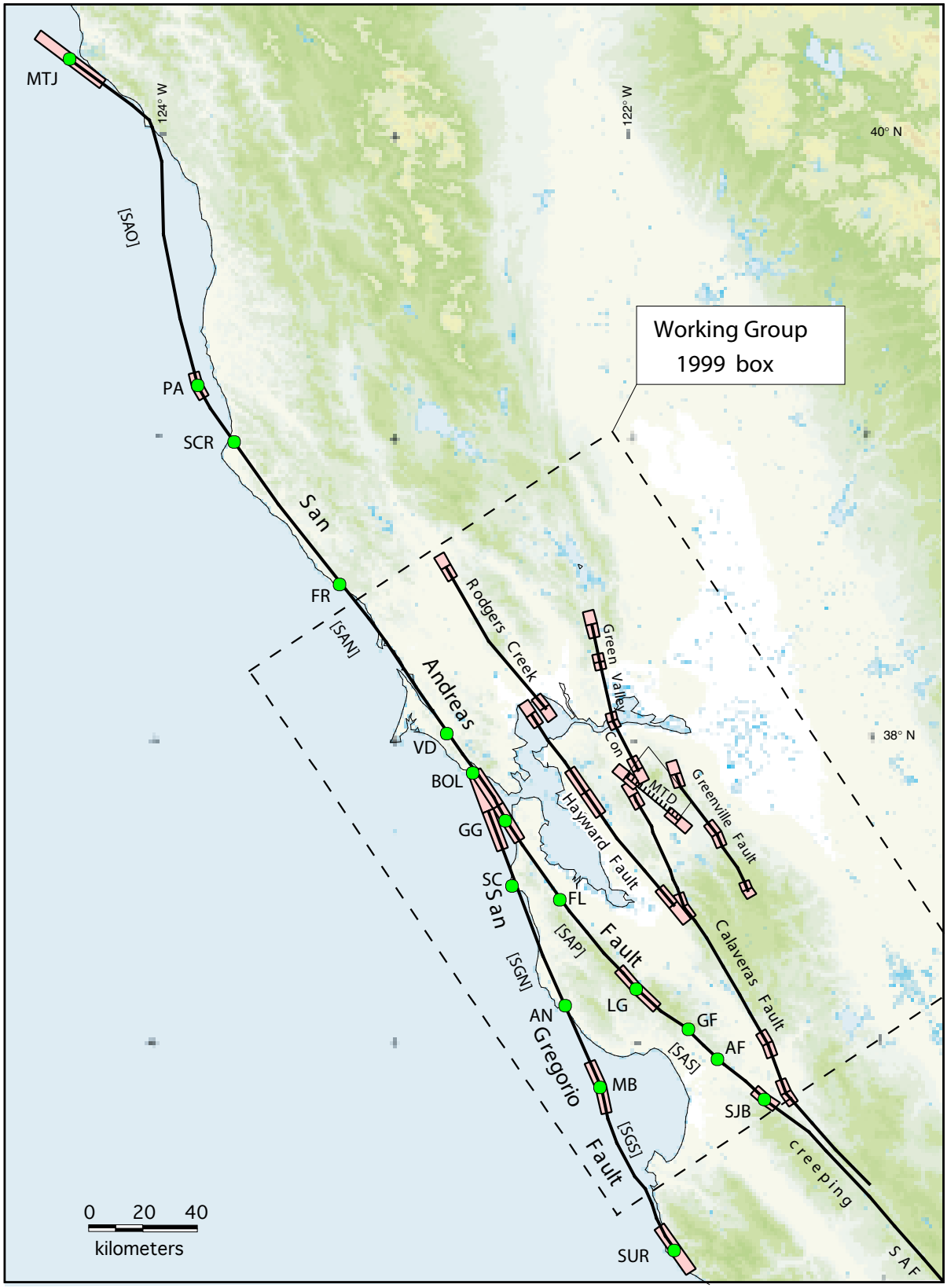

Figure 3.1. Segmentation of SFBR faults. Bold solid lines indicate major faults for which probabilities were calculated. Light rectangles are segment boundaries. *MTD*, Mount Diablo Thrust; *Con*, Concord Fault. San Andreas Fault segments: SAN, North Coast; SAO, Offshore; SAP, Peninsula; SAS, Santa Cruz Mountains. San Gregorio Fault segments: SGN,North; SGS, South. Localities (circles): AF, Arano Flat; AN, Ano Nuevo; BOL, Bolinas, FL, Filoli; FR, Fort Ross; GF, Grizzly Flat; GG, Golden Gate stepover zone in SAF and SGF; LG, Los Gatos bend in SAF; MB, Monterey bend in SGF; MTJ, Mendocino triple junction; PA, Point Arena; SC, Seal Cove; SCR, Scaramella Ranch; SJB, San Juan Bautista; SUR, Point Sur; VD, Vedanta.

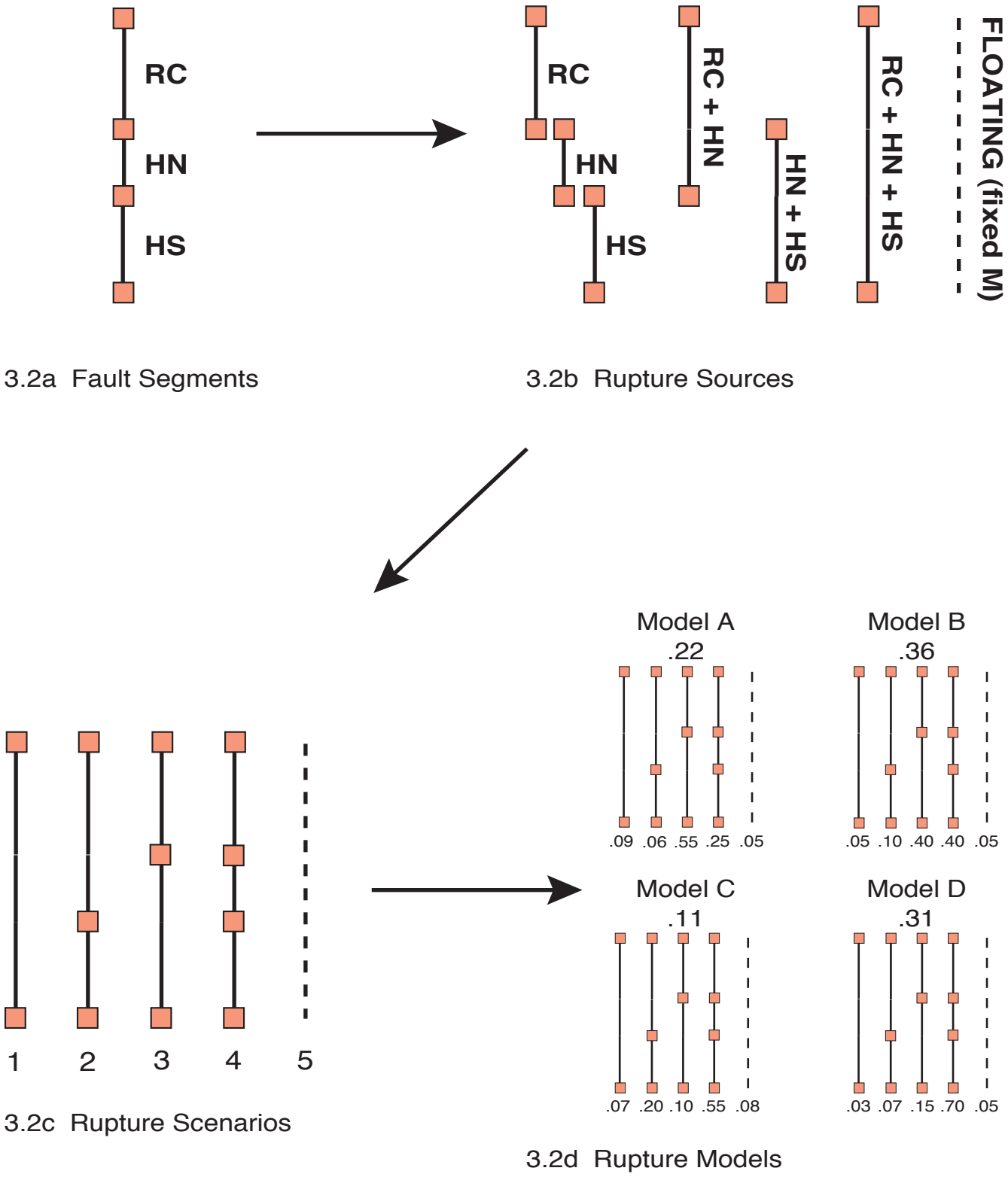

Figure 3.2 Diagram illustrating construction of rupture models from fault segments using the Hayward - Rodgers Creek fault as an example. Orange boxes are segment boudaries. a) initial 3-segment fault; b) 6 rupture sources (+ floating earthquake) derived from segments; c) rupture scenarios built from sources; d) rupture models with weights for each model and rupture scenario.

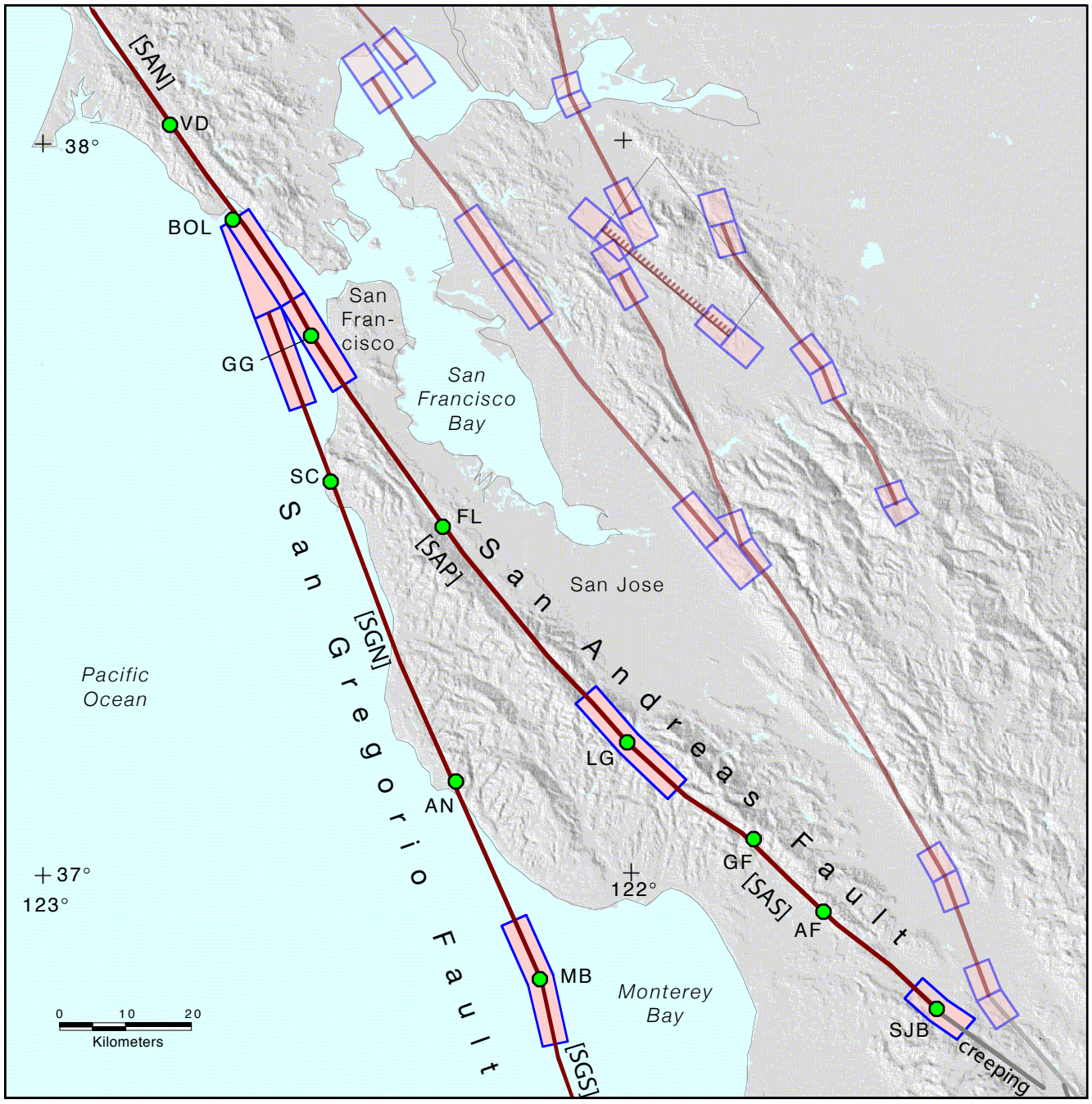

Figure 3.3. Segment boundaries for the San Andreas and San Gregorio faults. San Andreas Fault segments: SAN, North Coast; SAP, Peninsula; SAS, Santa Cruz Mountains. San Gregorio Fault segments: SGN, North; SGS, South. Localities (circles): AF, Arano Flat; AN, Ano Nuevo; BOL, Bolinas, FL, Filoli; GF, Grizzly Flat; GG, Golden Gate stepover zone in SAF and SGF; LG, Los Gatos bend in SAF; MB, Monterey bend in SGF; SC, Seal Cove; SJB, San Juan Bautista; VD, Vedanta.

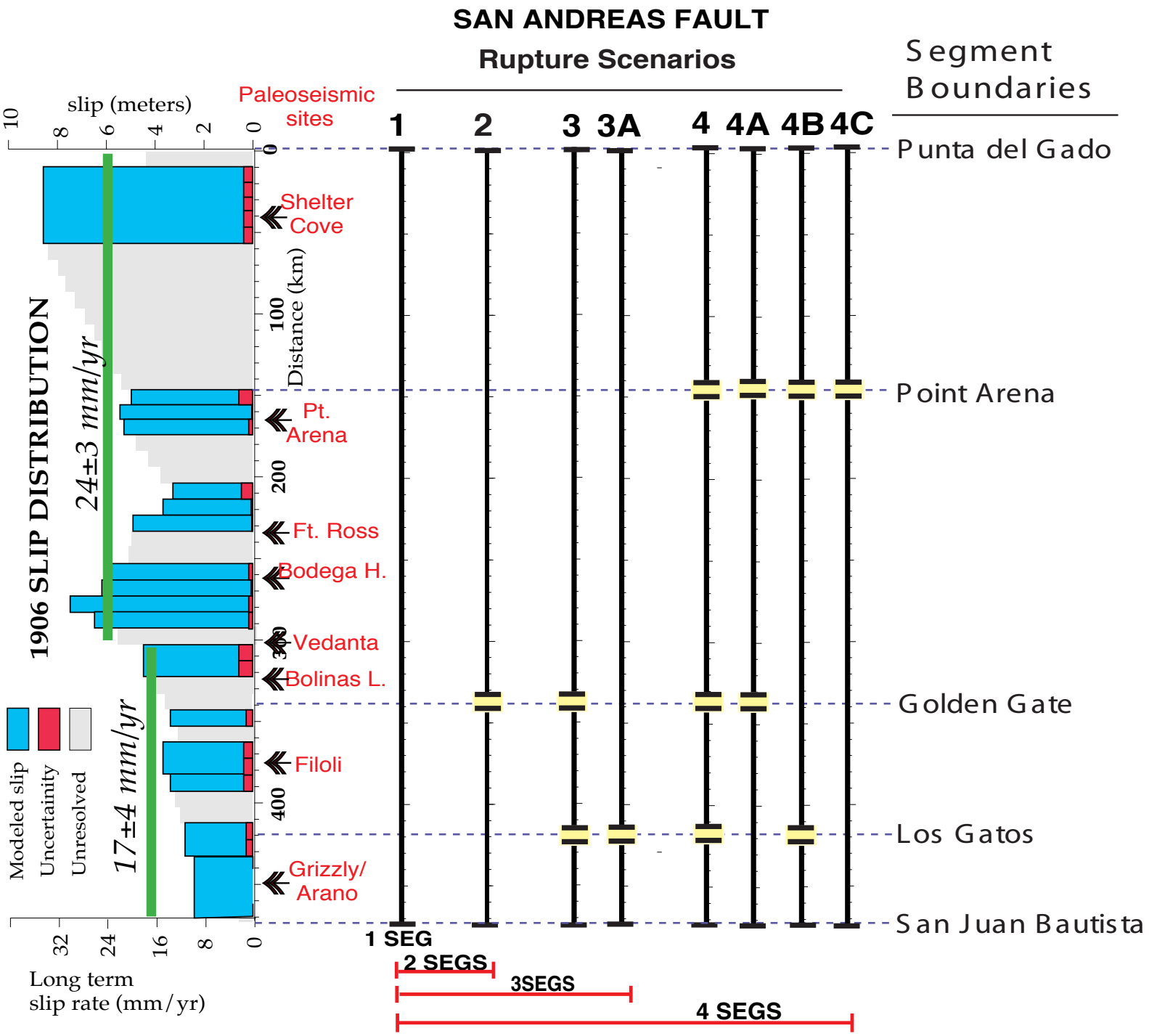

Figure 3.4 San Andreas rupture scenarios. Graph on left shows geodetic slip from 1906 earthquake. Green bands are geologic slip rates. Arrows show locations of paleoseismic sites described in text.

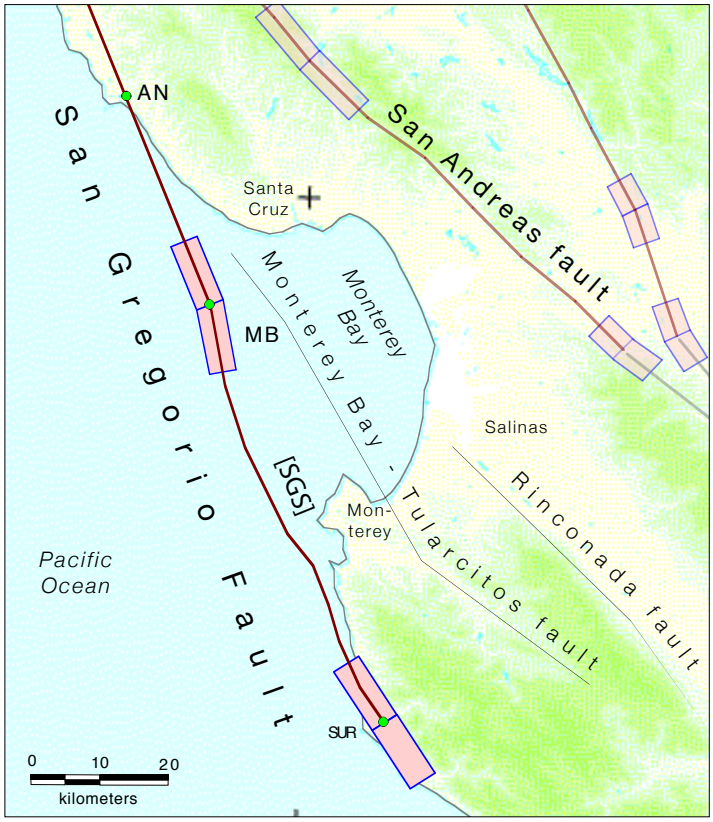

Figure 3.5. Segment boundaries for the southern segment of the San Gregorio fault [SGS]. Localities (circles): AN, Ano Nuevo; MB, Monterey bend in SGF; SUR, Point Sur.

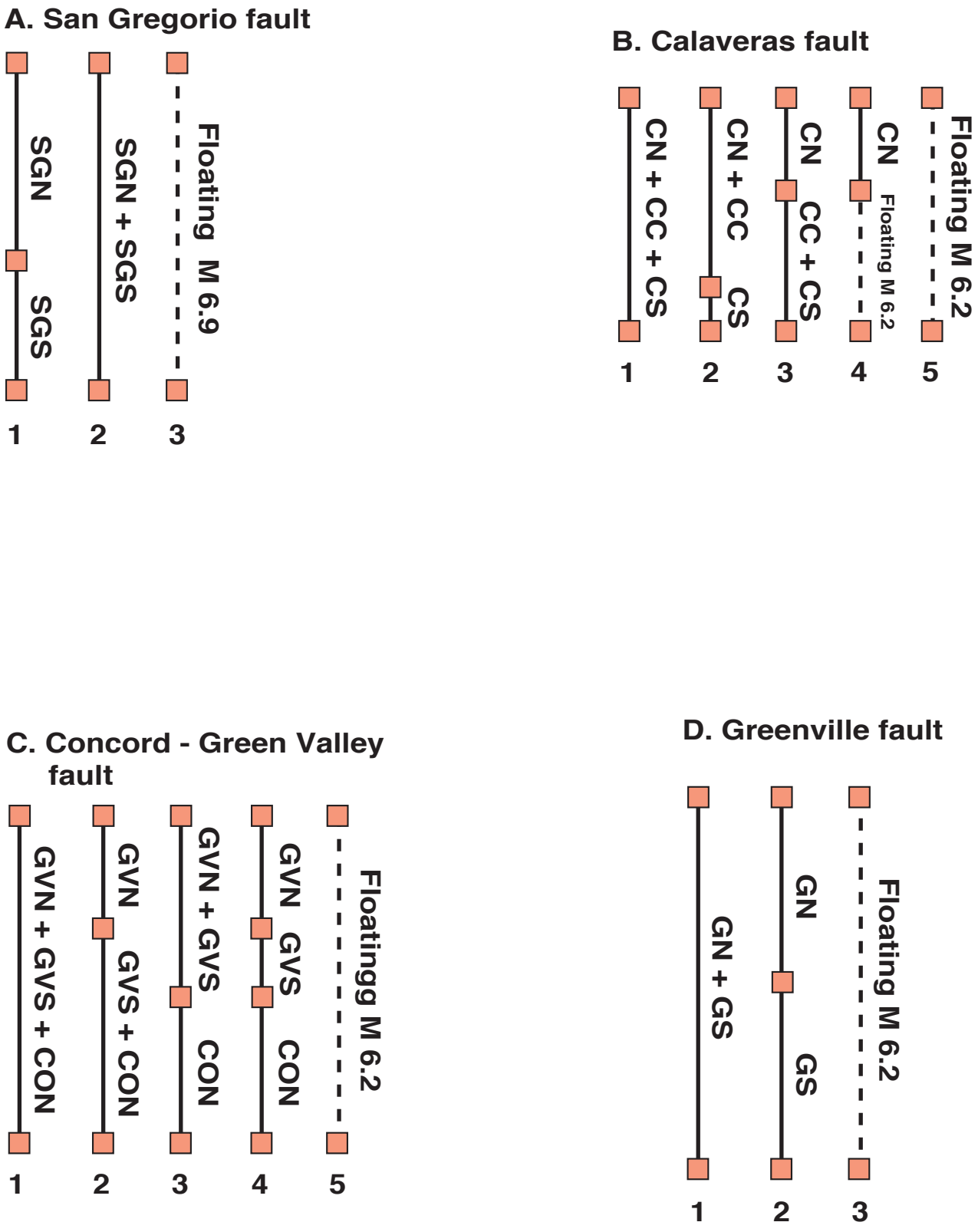

Figure 3.6 Schematic fault rupture scenarios for the San Gregorio (A), Calaveras (B), Concord - Green Valley (C), and Greenville (D) faults. Orange boxes are segment boundaries. Scenarios are described in text.

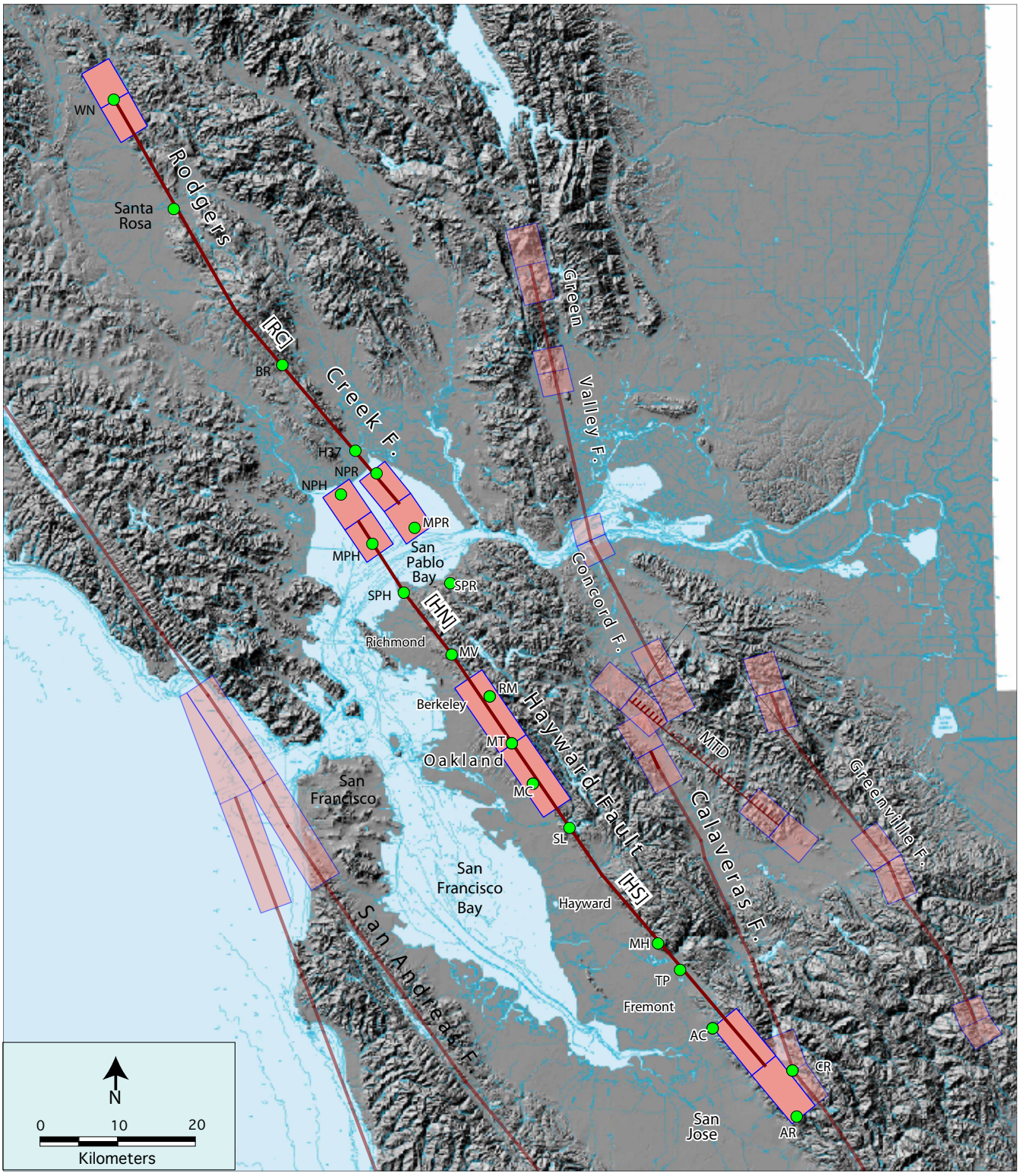

Figure 3.7. Hayward-Rogers Creek segments: HN, Hayward North; HS, Hayward South; RC, Rodgers Creek. AC, Agua Caliente Creek; AR, Alum Rock; BR, Beebe Ranch, CR; Calaveras Reservoir; H37, Highway 37; MC, Mills College; MH, Masonic Home; MPH, middle San Pablo Bay on Hayward fault; MPR, middle San Pablo Bay on Rodgers Creek fault; MT; Montclair; MV, Mira Vista Golf Course; NPH, north end San Pablo Bay on Hayward Fault; NPH, north end San Pablo Bay on Rodgers Creek Fault; RM, Rocky Mound; SL, San Leandro; SPH, south end San Pablo Bay on Hayward Fault; SPH, south end San Pablo Bay on Rodgers Creek Fault; TP, Tule Pond; WN, Windsor.

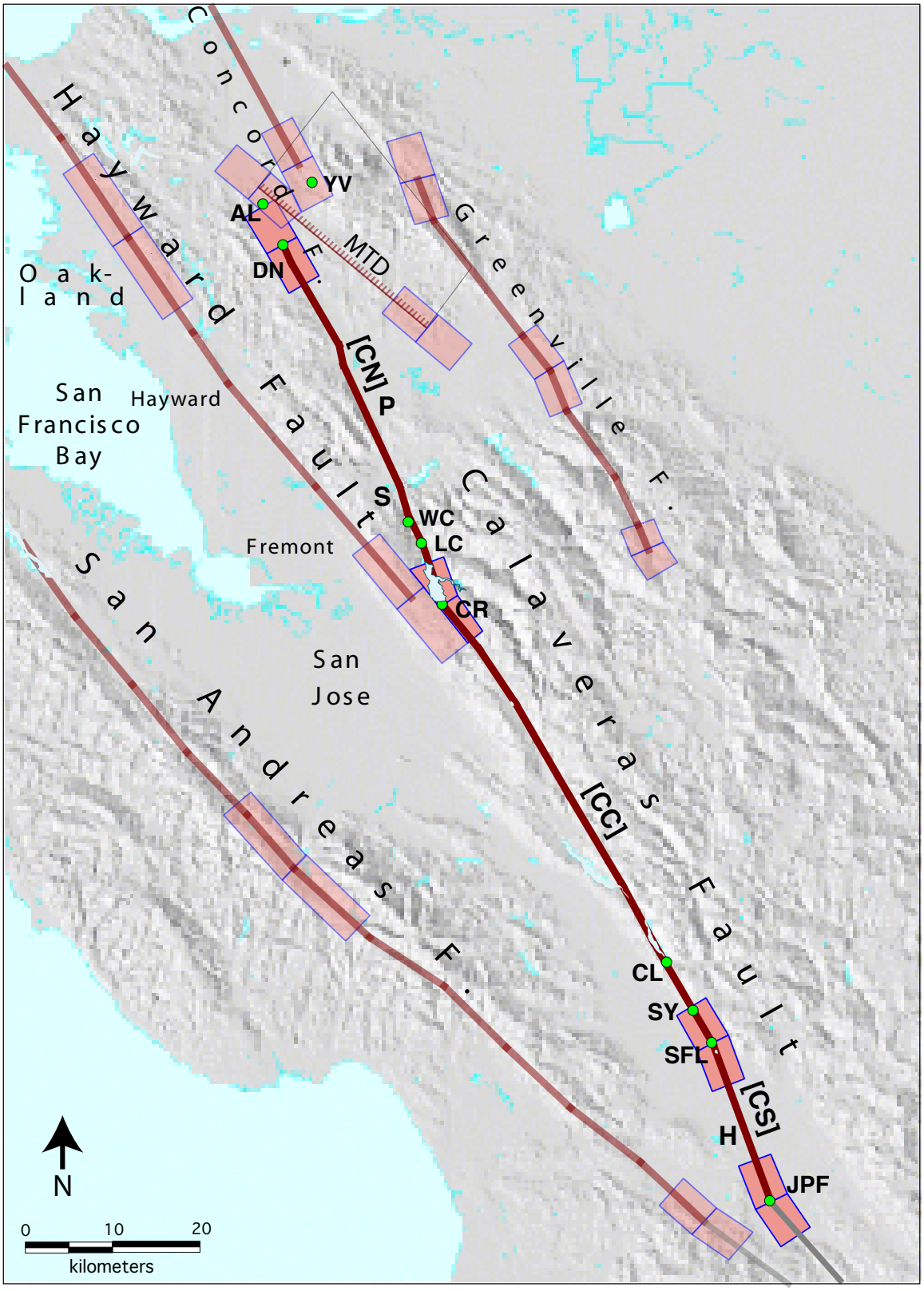

Figure 3.8. Calaveras Fault segments: CC, Central; CN, North; CS, South. Localities: AL, Alamo; CL,Coyote Lake; DN, Danville; H, Hollister; JPF, Junction Paicines Fault; LC, Leyden Creek; P, Pleasanton; S, Sunol; SFL, San Felipe Lake; SY, San Ysidro Creek; WC, Welch Creek; YV, Ygnacio Valley

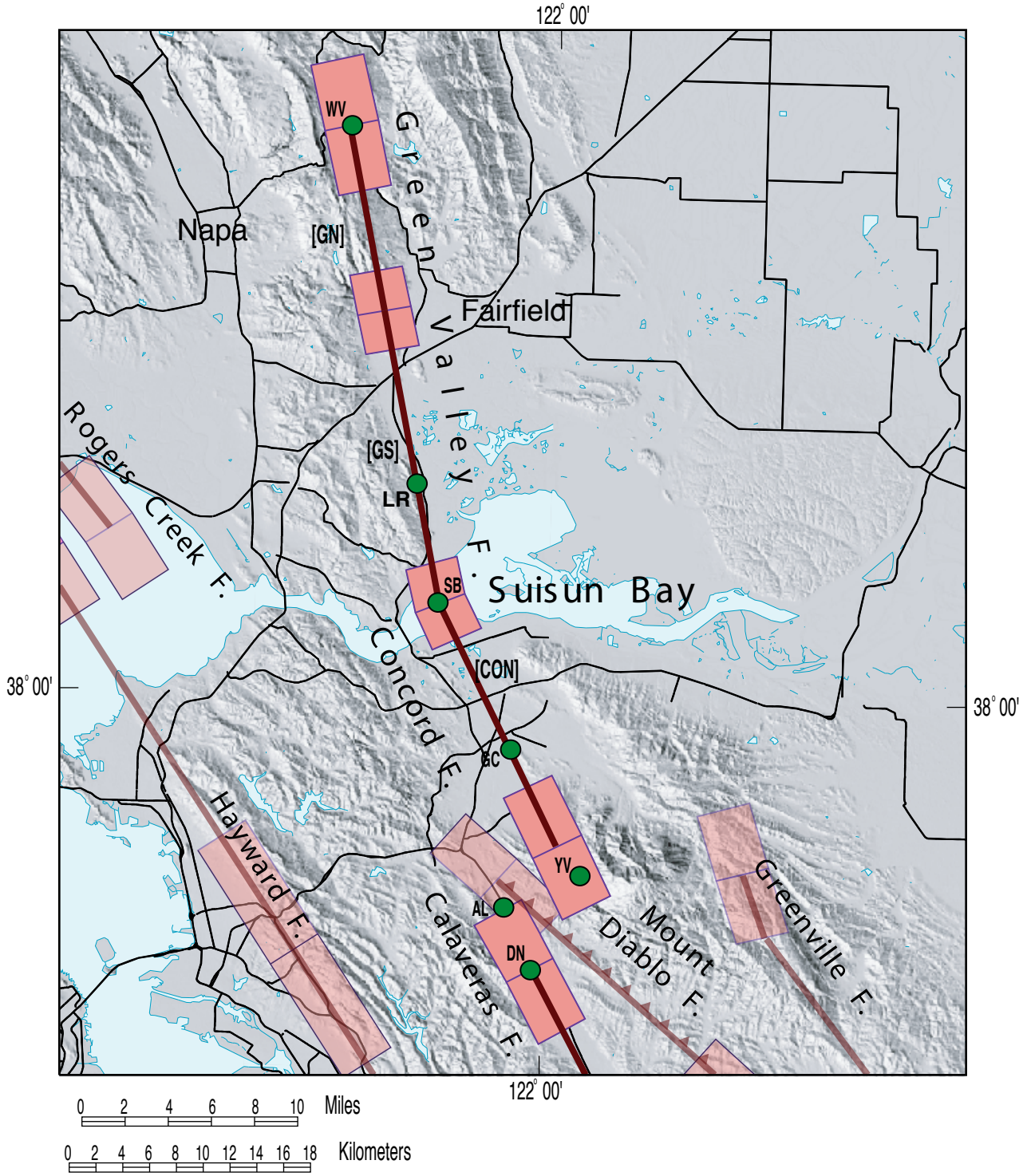

Figure 3.9. Segments of the Green Valley and Concord Faults. Segments: CON, Concord; GVN, Green Valley Fault North; GVS, Green Valley Fault South. Localities: GC, Gallindo Creek; LR, Lopes Ranch; SB, Suisun Bay; WV, Wooden Valley; Ygnacio Valley; others same as previous figures.

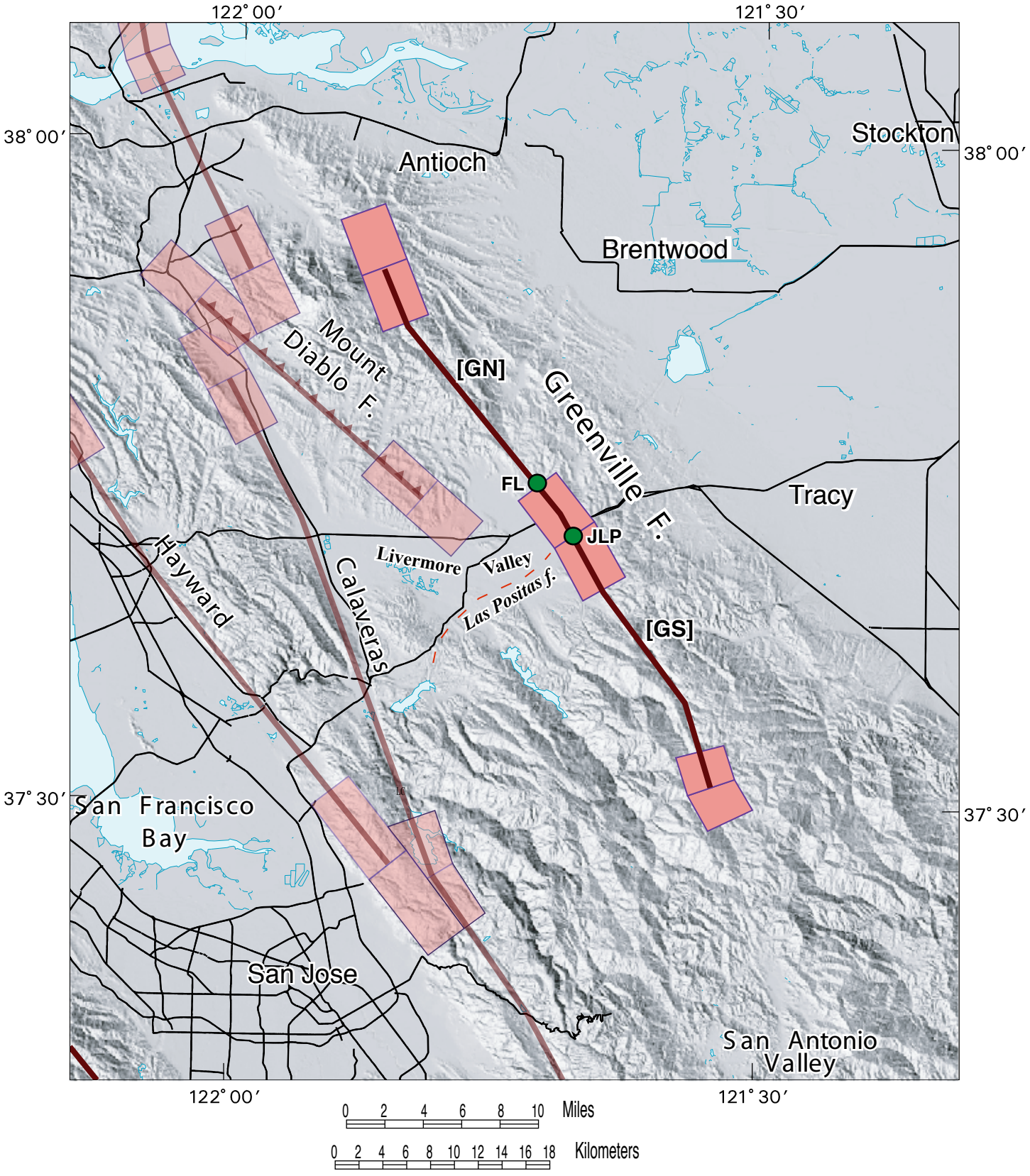

Figure 3.10. Segments of the Greenville fault: GN, North; GS, South. Localities: FL, Frick Lake; JLP, Junction Las Positas Fault.

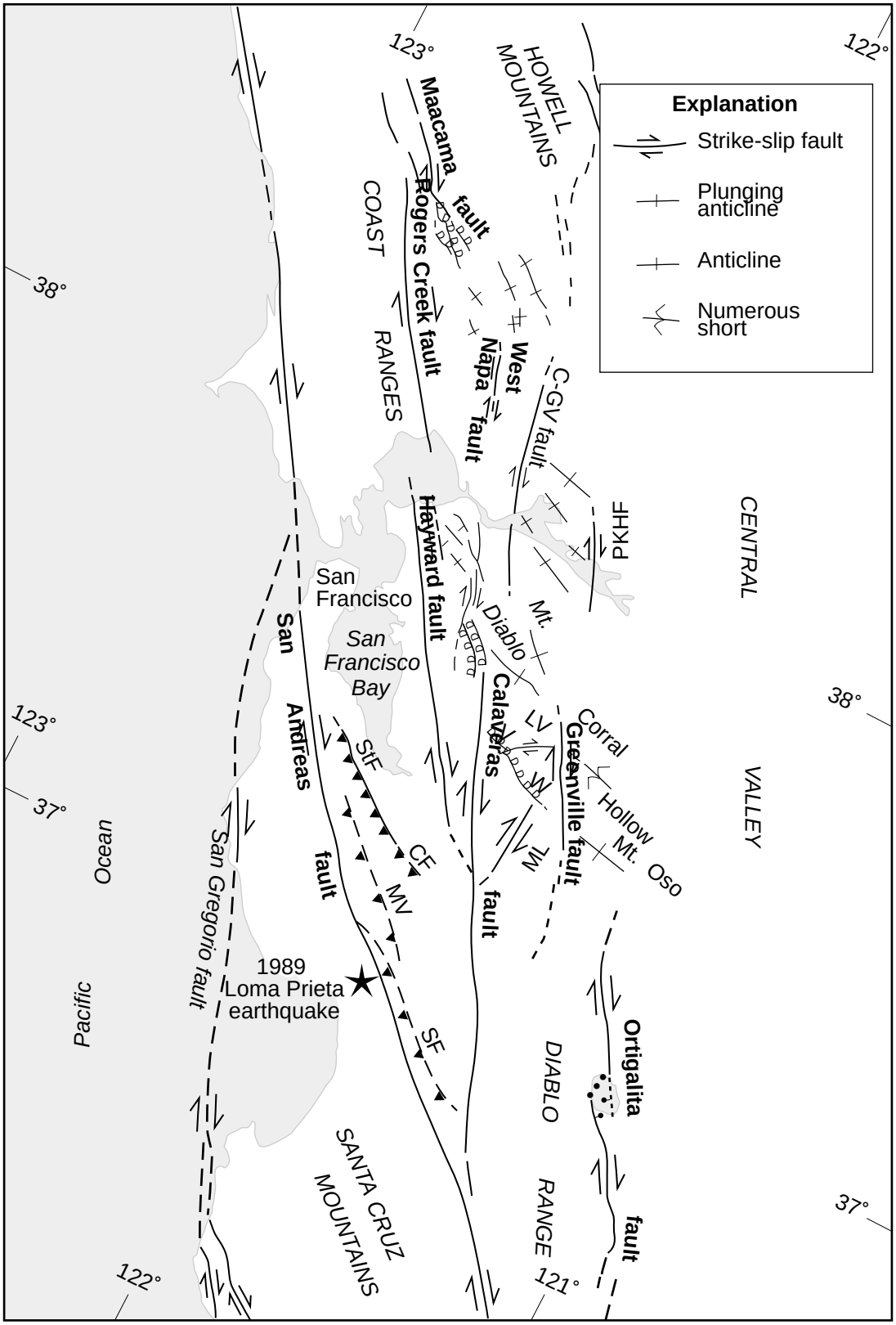

Figure 3.11. Major late Cenozoic strike-slip faults, folds and thrust faults in the greater San Francisco Bay area. Note that the thrust faults and folds typically are oriented about 45° to the strike-slip faults of the San Andreas system, and locally exhibit a right-stepping en echelon geometry typical of dextral wrench structures. Collectively, the strike-slip faults, thrust faults and folds accommodate about 40 mm/yr of NW dextral shear between the Pacific plate on the west and the Sierra Nevada-Great Valley microplate on the east. Abbreviations: StF = Stanford fault; CF = Cascade fault; MV = Monte Vista fault; SF = Sargent fault; LV = Livermore Valley; ML = Mt. Lewis fault; V = Verona fault; W = Williams fault; PKHF = Pittsburg-Kirby Hills fault.

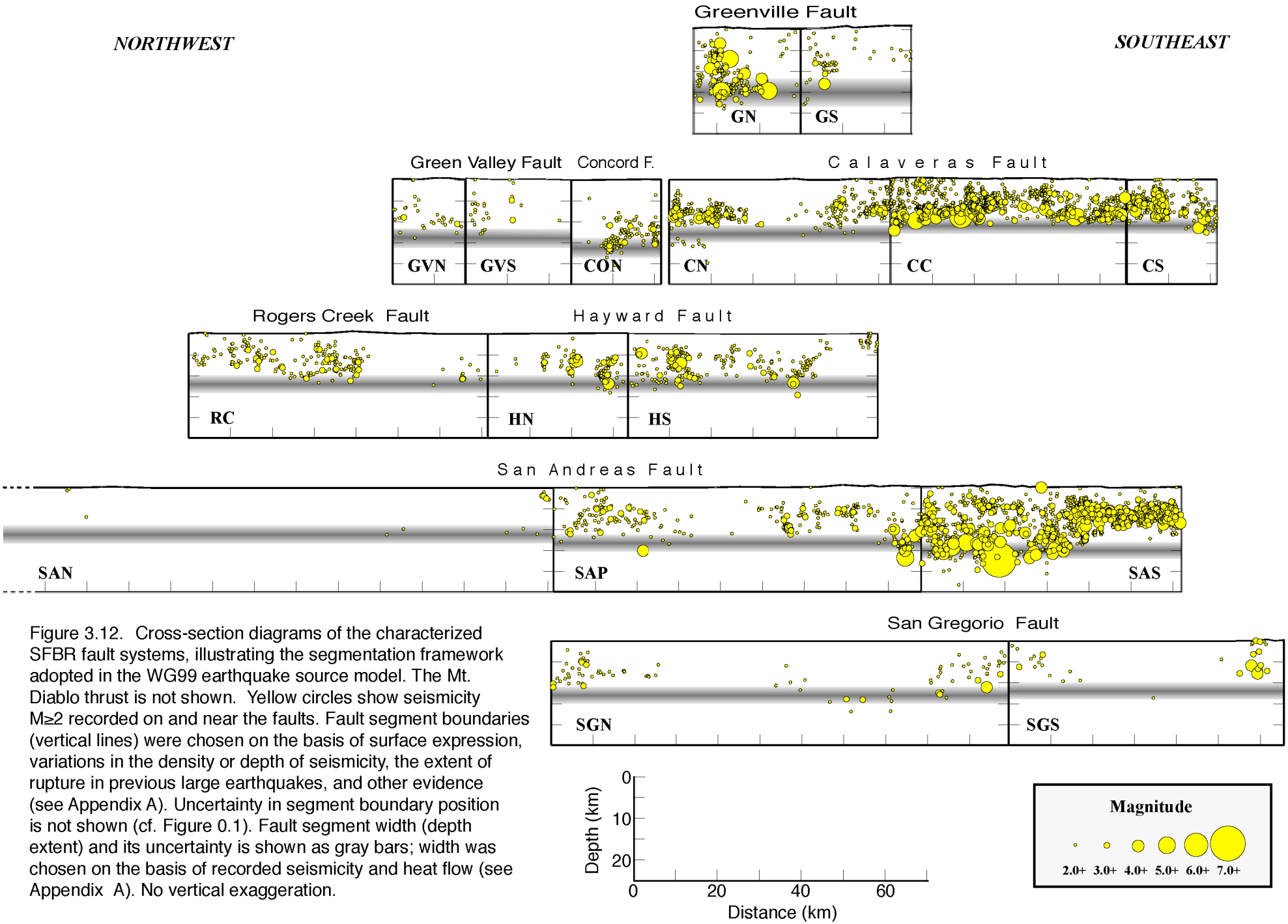

Figure 3.12. Cross-section diagrams of the characterized SFBR fault systems, illustrating the segmentation framework adopted in the WG99 earthquake source model. The Mt. Diablo thrust is not shown. Yellow circles show seismicity M≥2 recorded on and near the faults. Fault segment boundaries (vertical lines) were chosen on the basis of surface expression, variations in the density or depth of seismicity, the extent of rupture in previous large earthquakes, and other evidence (see Appendix A). Uncertainty in segment boundary position is not shown (cf. Figure 0.1). Fault segment width (depth extent) and its uncertainty is shown as gray bars; width was chosen on the basis of recorded seismicity and heat flow (see Appendix A). No vertical exaggeration.